

# Differential Temperature-Dependent Multimeric Assemblies of Replication and Repair Polymerases on DNA Increase Processivity

Hsiang-Kai Lin,<sup>†</sup> Susan F. Chase,<sup>‡</sup> Thomas M. Laue,<sup>‡</sup> Linda Jen-Jacobson,<sup>\*,§</sup> and Michael A. Trakselis<sup>\*,†</sup>

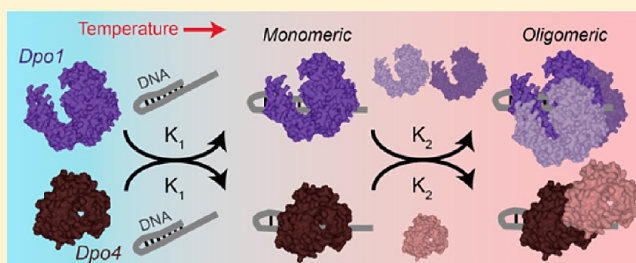
<sup>†</sup>Department of Chemistry, University of Pittsburgh, Pittsburgh, Pennsylvania 15260, United States

<sup>‡</sup>Department of Biochemistry, University of New Hampshire, Durham, New Hampshire 03824, United States

<sup>§</sup>Department of Biological Sciences, University of Pittsburgh, Pittsburgh, Pennsylvania 15260, United States

## S Supporting Information

**ABSTRACT:** Differentiation of binding accurate DNA replication polymerases over error prone DNA lesion bypass polymerases is essential for the proper maintenance of the genome. The hyperthermophilic archaeal organism *Sulfolobus solfataricus* (Sso) contains both a B-family replication (Dpo1) and a Y-family repair (Dpo4) polymerase and serves as a model system for understanding molecular mechanisms and assemblies for DNA replication and repair protein complexes. Protein cross-linking, isothermal titration calorimetry, and analytical ultracentrifugation have confirmed a previously unrecognized dimeric Dpo4 complex bound to DNA. Binding discrimination between these polymerases on model DNA templates is complicated by the fact that multiple oligomeric species are influenced by concentration and temperature. Temperature-dependent fluorescence anisotropy equilibrium binding experiments were used to separate discrete binding events for the formation of trimeric Dpo1 and dimeric Dpo4 complexes on DNA. The associated equilibria are found to be temperature-dependent, generally leading to improved binding at higher temperatures for both polymerases. At high temperatures, DNA binding of Dpo1 monomer is favored over binding of Dpo4 monomer, but binding of Dpo1 trimer is even more strongly favored over binding of Dpo4 dimer, thus providing thermodynamic selection. Greater processivities of nucleotide incorporation for trimeric Dpo1 and dimeric Dpo4 are also observed at higher temperatures, providing biochemical validation for the influence of tightly bound oligomeric polymerases. These results separate, quantify, and confirm individual and sequential processes leading to the formation of oligomeric Dpo1 and Dpo4 assemblies on DNA and provide for a concentration- and temperature-dependent discrimination of binding undamaged DNA templates at physiological temperatures.



Over the past two decades, a multitude of DNA polymerases have been discovered and classified into at least six separate families.<sup>1</sup> Many organisms have multiple DNA polymerases, with humans having 15.<sup>2</sup> Most traditional B-family DNA polymerases are involved in faithful copying of our genome, while Y-family DNA polymerases have more flexible active sites allowing for synthesis across locations of DNA damage in an effort to maintain uninterrupted DNA synthesis during replication. Binding and recognition of normal or damaged DNA bases require that each DNA polymerase have a precise specificity with the appropriate DNA template to maintain fidelity of replication or repair directed by interacting proteins at the replication fork. Specificity is increased through interactions with shared accessory proteins for DNA replication and repair polymerases at the site of catalysis. Alternatively, the repeated shuttling between polymerization and exonuclease states of B-family DNA polymerases at sites of damage<sup>3</sup> may locally destabilize binding, allowing a Y-family polymerase to bind more specifically to bypass the lesion. Therefore, a question of how each polymerase is regulated with regard to binding the correct DNA substrate arises.

DNA polymerases Klenow,<sup>4</sup> T4 gp43,<sup>5</sup> human pol  $\beta$ ,<sup>6,7</sup> and African swine fever virus polymerase X<sup>8</sup> have all been found to form 2:1 complexes with DNA.<sup>9</sup> Other DNA polymerases appear at the replication fork as multimers during DNA replication through interactions with their accessory proteins.<sup>10</sup> Interestingly, DNA replication polymerases have also been found to exchange freely from solution during active replication, suggesting that either direct interactions between polymerases or indirect interactions through accessory proteins provide mechanisms for switching enzymes at the site of catalysis.<sup>11,12</sup> Therefore, it is likely that the high concentration of DNA polymerases within or around replisome complexes is a common mechanism for coordinated DNA synthesis, increased kinetics, and coupled replication and repair for maintaining the genomic integrity of the cell.

DNA replication in archaea serves as an important and relevant model system for detailing the molecular mechanisms of DNA polymerases homologous to their eukaryotic counter-

Received: July 17, 2012

Revised: August 20, 2012

Published: August 21, 2012



parts.<sup>13–15</sup> Contained within the archaeal *Sulfolobus solfataricus* genome are DNA polymerases from both the B-family replication (Dpo1) and Y-family lesion bypass (Dpo4) families. Both individual DNA polymerases have been structurally characterized,<sup>16–18</sup> have similar specificities for DNA<sup>19,20</sup> and robust kinetics,<sup>21–23</sup> but differ in their fidelities for nucleotide incorporation.<sup>21,24–26</sup> Dpo4's lower fidelity, as well as the ability for *Sulfolobus* to survive in the absence of this protein,<sup>27</sup> highlights a nonessential role in DNA replication. Direct interaction between Dpo1 and Dpo4 has also been noted and is thought to be important for uninterrupted lesion bypass during DNA replication.<sup>28</sup> We have also shown that Dpo1 can form a trimeric complex in the presence of DNA,<sup>20</sup> suggesting that homo- and hetero-oligomeric DNA polymerase complexes exist.

Quantification of binding various DNA polymerases to DNA has been examined using a number of techniques to characterize this single binding event. The resulting temperature-dependent thermodynamic binding parameters can provide insight into the specificity of the binding process through determination of the heat capacity change ( $\Delta C_p^\circ$ ).<sup>29,30</sup> Although a strongly negative  $\Delta C_p^\circ$  has been shown to be the thermodynamic signature of sequence-specific binding,<sup>30</sup> the non-sequence-specific binding to primer–template DNA by the A-family DNA polymerases from *Thermus aquaticus* (Taq)<sup>31</sup> and *Escherichia coli* (Klenow)<sup>32</sup> is also associated with large and negative  $\Delta C_p^\circ$  values.<sup>29,33–35</sup> Even though there is no sequence specificity, the negative  $\Delta C_p^\circ$  is consistent with the high degree of structural complementarity<sup>29</sup> of the DNA polymerase binding to the primer–template junction, visualized in a variety of crystal structures.<sup>18,36,37</sup> The inherent thermostability of proteins from *Sso* (where the growth temperature is  $\sim 75^\circ\text{C}$ ) allows us to fully investigate the energetic constraints of DNA polymerase binding to DNA. Access to this broad temperature range results in a more complete thermodynamic characterization of the differences in binding of B- and Y-family polymerases to an undamaged DNA primer–template. These thermodynamic differences can be evaluated directly by determining the affinities ( $K_d$ ), free energies ( $\Delta G^\circ$ ), heat capacity changes ( $\Delta C_p^\circ$ ), and stoichiometries ( $n$ ) for binding each polymerase.

Here, we use chemical cross-linking, isothermal calorimetry (ITC), and analytical ultracentrifugation (AUC) to show that Dpo4, like Dpo1, can also form an oligomeric complex on DNA. Using AUC, we have found both a strong concentration-dependent and modest temperature-dependent shift in the reaction boundaries, highlighting changes in Dpo4 monomer–dimer and Dpo1 monomer–trimer equilibria. Temperature-dependent equilibrium fluorescent anisotropy binding experiments were used to separate the free energy ( $\Delta G^\circ$ ) of binding either monomer or higher-order oligomeric DNA polymerase (Dpo1 or Dpo4) states. For both polymerases, we have detected an initial higher-affinity monomeric binding site followed by sequential binding of additional polymerase molecules to form either trimeric Dpo1 or dimeric Dpo4 complexes on DNA. Separation and quantification of these individual binding events reveal that a Dpo1 monomer binds to DNA with an only slightly greater affinity than Dpo4 up to  $50^\circ\text{C}$ . This binding affinity difference is exaggerated at the highest temperatures, suggesting that binding of Dpo1 to undamaged DNA templates is favored under physiological growth conditions for *Sso*. The free energy associated with trimer Dpo1 binding to DNA is significantly more favorable than that

associated with dimer Dpo4 binding to DNA, and this difference increases strongly with an increase in temperature. Enzymatic evidence showing greater processivities for Dpo1 and Dpo4 at higher temperatures and protein concentrations is used to explain the role of temperature and oligomeric state in promoting DNA polymerase assembly, stability, and kinetics at the replication fork. Collectively, our results indicate that the binding specificities of multiple oligomeric archaeal DNA polymerases are regulated by changes in cellular concentrations and temperature for efficient DNA binding recognition and synthesis.

## EXPERIMENTAL PROCEDURES

**Materials.** Oligonucleotide substrates, including the 37-nucleotide (nt) DNA hairpin, 5'-fluorescein, or 5'-Cy3-labeled DNA, were purchased from Integrated DNA Technologies (IDT, Coralville, IA). The sequence of the 37-nucleotide DNA hairpin was 5'-TTTTTTTTTCCCGGGCCGCGTTTCG-CCGGCCCCGGG, which included a 12 bp duplex region, a three-residue loop, and a 10-residue single-strand template. DNA was dissolved in annealing buffer [20 mM HEPES (pH 7) and 200 mM NaCl], heated to  $95^\circ\text{C}$  for 15 min, and then cooled to room temperature because the hot plate was turned off overnight. M13mp18 was purchased from USB Corp. (Cleveland, OH). All radiochemicals were purchased from MP Biochemicals (Santa Ana, CA) or Perkin-Elmer (Waltham, MA). Commercial enzymes were from NEB (Ipswich, MA). All other chemicals were analytical grade or better.

Dpo1 and Dpo4 were purified as described previously<sup>17,20</sup> except for a few modifications. The exonuclease deficient version of Dpo1 (D231A/D318A) was recloned into pET30a (*NdeI/XhoI*) to introduce a stop codon and remove the C-terminal His tag. Both polymerases were expressed using an autoinduction protocol<sup>38</sup> using Rosetta 2 cells (Stratagene). Cells were lysed by sonication and heat treated at  $70^\circ\text{C}$  for 30 min followed by centrifugation. The Dpo1 lysate was purified using HiTrap MonoQ, heparin, and Superdex-200 gel filtration columns. The wild-type untagged Dpo4 lysate was purified using HiTrap MonoQ, heparin, and hydroxylapatite (Sigma-Aldrich) columns.<sup>17</sup>

**Cross-Linking Studies.** Dpo4 was dialyzed in cross-linking buffer [50 mM HEPES (pH 7.0), 150 mM NaCl, and 10 mM EDTA] and reduced using 10 mM tris(2-carboxyethyl)-phosphine hydrochloride (TCEP-HCl) (Thermo Scientific, Rockford, IL). Dpo4 (8  $\mu\text{M}$ ) was then incubated either alone or with 10  $\mu\text{M}$  DNA 37-nucleotide hairpin for 5 min at room temperature. Chemical cross-linking experiments were initiated with 0.33 mM 1,11-bis-maleimidotriethylene glycol [BM-(PEG)<sub>3</sub>] or ethylene glycol bis(succinimidylsuccinate) (EGS) (Pierce, Rockford, IL) targeting free cysteines or free amines, respectively, in the proximity. The reaction mixture was then incubated for 15 min at  $22^\circ\text{C}$ . Products were separated on an 8% sodium dodecyl sulfate–polyacrylamide gel electrophoresis (SDS–PAGE) gel and stained with Coomassie dye.

**Isothermal Titration Calorimetry (ITC).** Prior to analysis, titrants and analytes were dialyzed against buffer A [20 mM HEPES–NaOH (pH 7), 150 mM NaCl, 5% glycerol, 10 mM Mg(OAc)<sub>2</sub>, and 0.2 mM DTT], filtered by centrifuge tube filters (0.22  $\mu\text{M}$ , SPIN-X, Corning Inc., Corning, NY), and degassed. Isothermal titration calorimetry was performed using a VP-ITC instrument (MicroCal Inc., Northampton, MA) as described previously.<sup>20</sup> Titrations were performed by titrating 400  $\mu\text{M}$  37-nucleotide hairpin (primer–template hairpin) (5–8

$\mu\text{L}$  aliquots) into 25  $\mu\text{M}$  Dpo4 at 15 or 60  $^{\circ}\text{C}$ . The heats of the reaction were corrected for the heat of dilution by subtracting the signal after saturation had been reached. All data were fit using Origin 7.0 (MicroCal) according to the following equation:

$$Q = \frac{n[M]_t \Delta H^{\circ} V_0}{2} \left\{ 1 + \frac{[L]_t}{n[M]_t} + \frac{1}{nK_a[M]_t} - \left[ \left( 1 + \frac{[L]_t}{n[M]_t} + \frac{1}{nK_a[M]_t} \right)^2 - \frac{4[L]_t}{n[M]_t} \right]^{1/2} \right\} \quad (1)$$

where  $V_0$  is the volume of the cell,  $\Delta H^{\circ}$  is the enthalpy of binding per mole of ligand,  $[M]_t$  is the concentration of DNA, including both bound and free fractions,  $K_a$  is the association constant,  $[L]_t$  is the total ligand (Dpo4) concentration, and  $n$  is the stoichiometry of the reaction.<sup>20,39</sup>

**Analytical Ultracentrifugation (AUC) Sedimentation Velocity Experiments.** Sedimentation velocity experiments were performed using an Optima XLI analytical ultracentrifuge (Beckman Coulter, Fullerton, CA) equipped with a prototype fluorescence optical system (Aviv Biomedical). Samples of protein alone or with (50 nM) fluorescein-labeled 37-nucleotide hairpin (primer–template) DNA in buffer A were loaded into ultracentrifuge cells at various concentrations (0, 10, 50, 100, 200, 500, 1000, 2000, 5000, and 10000 nM) into a double-sector charcoal-Epon centerpiece in a four- or eight-hole titanium rotor and subjected to an angular velocity of 45000 rpm with a temperature of 10, 20, or 30  $^{\circ}\text{C}$ . Absorbance or fluorescence scans as a function of radial position were collected by scanning at 280 nm (protein alone) or 488 nm (protein with fluorescein DNA) at 20  $\mu\text{m}$  radial increments, averaging three revolutions per scan. Sedimentation velocity boundaries were analyzed in the least-squares sedimentation coefficient distribution [ls-g\*(s)] model using SEDFIT (version 12.1).<sup>40</sup> The sedimentation coefficient,  $s$ , is given by Svedberg's equation:

$$s = \frac{M_w D_t (1 - \bar{v} \rho)}{RT} \quad (2)$$

where  $M_w$  is the molecular weight,  $D_t$  is the diffusion coefficient,  $\bar{v}$  is the partial specific volume,  $\rho$  is the solvent density,  $R$  is the universal gas constant, and  $T$  is the temperature. Observed weight average sedimentation coefficients were converted to  $s_{20,w}$  (standard conditions of 20  $^{\circ}\text{C}$  in water), accounting for partial specific volumes, buffer densities, and viscosities, calculated using SEDNTERP.<sup>41,42</sup>

**Fluorescence Anisotropy, Equilibrium Binding, and Thermodynamic Parameters.** A 5'-Cy3-labeled 37 nt hairpin primer–template DNA construct, described previously,<sup>20</sup> was used in the fluorescence anisotropy experiments. Titrations were performed in buffer A using a fixed concentration of DNA (4 nM) and varying concentrations of protein (0–20  $\mu\text{M}$ ). Anisotropy measurements were performed using a FluoroMax-3 spectrofluorimeter (HORIBA Jobin Yvon) equipped with automated polarizers and regulated with a thermostated cuvette holder. The DNA and protein were allowed to equilibrate at each temperature for at least 30 min prior to the measurement of the anisotropy. Titrations at higher temperatures (>45  $^{\circ}\text{C}$ ) were performed in a capped cuvette to limit changes in concentration caused by evaporation.

Fluorescence was excited at 550 nm, and the emission with various combinations of polarizers was monitored at 564 nm during a 5 s integration time. The fluorescence anisotropy,  $r$ , was calculated automatically by the instrumental software using the equation

$$r = \frac{I_{VV} - GI_{VH}}{I_{VV} + 2I_{VH}} \quad (3)$$

where  $I$  is the polarized fluorescence intensity with subscripts V and H identifying vertically and horizontally polarized light, respectively. The  $G$  factor is a correction for the difference in sensitivities of detection for horizontally and vertically polarized light. In all titrations, protein was titrated into DNA. After each addition, the protein was equilibrated until no further change in anisotropy was detected, generally 1 min. The fluorescence intensity of Cy3 is known to change with temperature.<sup>43</sup> Therefore, the slits were adjusted accordingly at each temperature to give a total fluorescence signal of approximately  $10^6$  counts per second for each titration. As a control for specific binding, the absolute fluorescence intensity at 564 nm did not change significantly upon addition of a high concentration of either Dpo1 or Dpo4 measured at the beginning and end of the experiment.

Anisotropy data were fit to either a single-binding site equation

$$\nu = \frac{A[P]}{K_d + [P]} \quad (4)$$

or a sequential-binding site equation

$$\nu = \frac{A_1[P]}{K_{d1} + [P]} + \frac{A_2[P]^n}{K_{d2}^n + [P]^n} \quad (5)$$

where  $A$  is the change in anisotropy,  $P$  is either the Dpo1 or Dpo4 concentration,  $K_d$  is the dissociation constant for each binding event (subscript 1 or 2), and  $n$  is the stoichiometry (2 for Dpo1 and 1 for Dpo4). At least three independent titrations were performed at each temperature to yield average  $K_{d1}$  and  $K_{d2}$  parameters.  $K_{d1}$  and  $K_{d2}$  were used to directly calculate the free energy change ( $\Delta G^{\circ}$ ) for the monomer

$$\Delta G^{\circ} = -RT \ln K_1 \quad (6)$$

and oligomer (Dpo1 trimer or Dpo4 dimer)

$$\Delta G^{\circ} = -RT \ln K_1 - nRT \ln K_2 \quad (7)$$

where  $R$  is the universal gas constant and  $T$  is the temperature.

Thermodynamic parameters were extracted from the temperature dependence of the Gibbs–Helmholtz plot from a multiparametric fit according to the following equations

$$\Delta G^{\circ} = \Delta H^{\circ} - T \Delta S^{\circ} = \Delta C_p^{\circ} \left[ T - T_H - T \ln \left( \frac{T}{T_S} \right) \right] \quad (8)$$

$$\Delta H^{\circ} = \Delta C_p^{\circ} (T - T_H) \quad (9)$$

$$\Delta S^{\circ} = \Delta C_p^{\circ} \ln \left( \frac{T}{T_S} \right) \quad (10)$$

where  $\Delta G^{\circ}$  is the standard free energy change,  $\Delta H^{\circ}$  is the change in enthalpy, and  $\Delta S^{\circ}$  is the change in entropy, using a constant change in heat capacity ( $\Delta C_p^{\circ}$ ) at each temperature  $T$ .



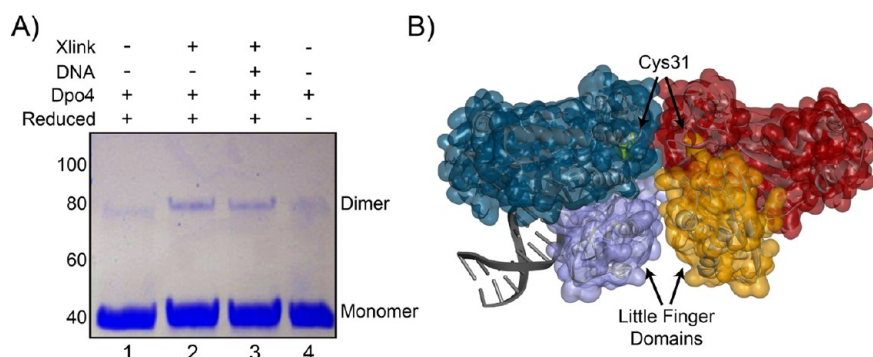


**Figure 1.** Dimeric Dpo4 complex formation. (A) Covalent protein cross-linking of Dpo4 in the absence and presence of a DNA hairpin or thiol–thiol cross-linker [BM(PEG)<sub>3</sub>]: lane 1, reduced Dpo4; lane 2, reduced Dpo4 with the cross-linker; lane 3, reduced Dpo4–DNA complex (37 nt hairpin) with the cross-linker; lane 4, unreduced Dpo4. The positions corresponding to monomer (40 kDa) and dimer (80 kDa) forms of Dpo4 are shown in the right margin. (B) X-ray structure of one possible dimeric Dpo4 conformation found in the crystal unit (PDB entry 2W9B) consistent with cross-linking at the C31 interface between molecules. Highlighted in purple and orange surfaces are the little finger domains from each Dpo4 molecule.

$T_H$  is the temperature at which  $\Delta H^\circ = 0$ , and  $T_S$  is the temperature at which  $T\Delta S^\circ = 0$ .

The binding data were also fit to a van't Hoff plot of  $\ln K_{app}$  versus  $1000/T$  according to the following equation

$$\ln K_{app} = \frac{\Delta C_p^\circ}{R} \left[ \frac{T_H}{T} - \ln \left( \frac{T_S}{T} \right) - 1 \right] \quad (11)$$

where  $K_{app}$  is the apparent equilibrium constant and  $R$  is the universal gas constant.

**Buried Surface Area Calculations.** Solvent accessible surface areas for Dpo4 bound to DNA [Protein Data Bank (PDB) entry 2RDJ]<sup>44</sup> were calculated for buried nonpolar ( $\Delta A_{np}$ ) and polar ( $\Delta A_p$ ) surface areas using a 1.4 Å probe radius as described previously.<sup>45</sup> The heat capacity change  $\Delta C_p^{SA}$  associated with binding was calculated from a surface area-based model according to Spolar et al.<sup>46</sup>

$$\Delta C_p^{SA} \text{ (cal mol}^{-1} \text{ K}^{-1}) = -0.32\Delta A_{np} + 0.14\Delta A_p \quad (12)$$

**Polymerase–DNA Binding Simulations.** The cumulative binding data for Dpo1 and Dpo4 were fit and modeled according to the minimal kinetic scheme outlined in panels A and B of Figure 7 using a simulation with Berkeley Madonna (University of California, Berkeley, CA) (see the Supporting Information for a full description of the parameters and equations used).

**DNA Polymerase Processivity.** Processivity experiments with Dpo1 and Dpo4 were performed and analyzed as previously described<sup>20</sup> but at additional temperatures. The 5′-<sup>32</sup>P end labeling of a DNA primer was performed using Optikinase (USB) and [ $\gamma$ -<sup>32</sup>P]ATP according to the manufacturer's directions. Primed M13mp18 DNA template (40 nM) was preincubated with various concentrations of Dpo1 or Dpo4 (as indicated in the figure legends) at the experimental temperatures in buffer A, and the reaction was initiated with the addition of dNTPs (0.1 mM each) and/or 30  $\mu$ g of single-strand salmon sperm DNA (Invitrogen, Carlsbad, CA). One volume of stop solution [50 mM NaOH, 1 mM EDTA, 3% (w/v) Ficoll (Type 400, Pharmacia), 0.05% (w/v) bromocresol green, and 0.04% (w/v) xylene cyanol] was added to terminate the processivity reactions after 60 min at 40 °C, 30 min at 50 °C, and 10 min at 60 or 70 °C. Aliquots were run on an alkaline agarose gel (0.8% agarose, 50 mM NaOH, and 1 mM EDTA) or denaturing 20% PAGE gel, dried, and imaged using a Storm

Phosphorimager (GE Healthsciences). Quantification of the mean band lengths was performed using ImageQuant version 5.0 compared with a <sup>32</sup>P end-labeled 1 kb ladder (Invitrogen).

## RESULTS

**Detection of Dimeric Dpo4.** After purifying Dpo4, we noticed a small amount of protein consistent with a covalent dimer on SDS–PAGE gels, especially under nonreducing conditions. We investigated the validity of a possible Dpo4 dimer using protein cross-linking. Chemical cross-linker BM(PEG)<sub>3</sub>, which targets native reduced cysteines, or EGS, which targets free amines in the proximity (<18 Å), was used to capture a dimer in solution. Dpo4 contains a single native cysteine residue (C31) that allows for the possibility of inferring information about the structure of a cross-linked species. Using the thiol–thiol cross-linker [BM(PEG)<sub>3</sub>], we were able to cross-link a dimeric Dpo4 in the absence and presence of DNA (Figure 1A, lanes 2 and 3). There is no significant difference in the amount of cross-linked Dpo4 complex in the presence of DNA. Therefore, a monomer–dimer equilibrium exists both on and off DNA. Unreduced Dpo4 loaded onto the SDS–PAGE gel also shows a small quantity of dimeric product, suggesting that a disulfide bond can form between subunits without an added cross-linker (Figure 1, lane 4). Reduction of this disulfide bond with TCEP reduces the fraction of dimer in favor of monomer (Figure 1, lane 1). We were also able to detect an equivalent reduced dimeric Dpo4 species using an amino–amino cross-linker (EGS) that cross-links lysine residues in an interface (data not shown). These cross-linking results suggest that dimeric Dpo4 complexes can exist in solution and that at least one conformation positions the single cysteine residue at the protein–protein interface, similar to that observed in an X-ray structure of Dpo4 bound to DNA (Figure 1B).<sup>47</sup>

**Stoichiometry of Binding of Dpo4 to DNA by Isothermal Titration Calorimetry.** To verify that a dimeric Dpo4 complex can exist on DNA over a broad temperature range, we used ITC to quantify the thermodynamics and stoichiometry of binding at 15 and 60 °C (Figure 2). At 15 °C, binding is primarily entropically driven, and a fit of the binding isotherm to eq 1 gave the following values:  $K_{app} = (6.5 \pm 0.6) \times 10^5 \text{ M}^{-1}$ ,  $\Delta H_{ITC}^\circ = 8.1 \pm 0.2 \text{ kcal mol}^{-1}$ , and  $n = 0.64 \pm 0.01$ . The resulting  $\Delta G_{ITC}^\circ$  is  $-7.7 \text{ kcal mol}^{-1}$ , and the calculated entropic contribution ( $T\Delta S_{ITC}^\circ$ ) is  $15.7 \text{ kcal mol}^{-1}$ . At 60 °C,

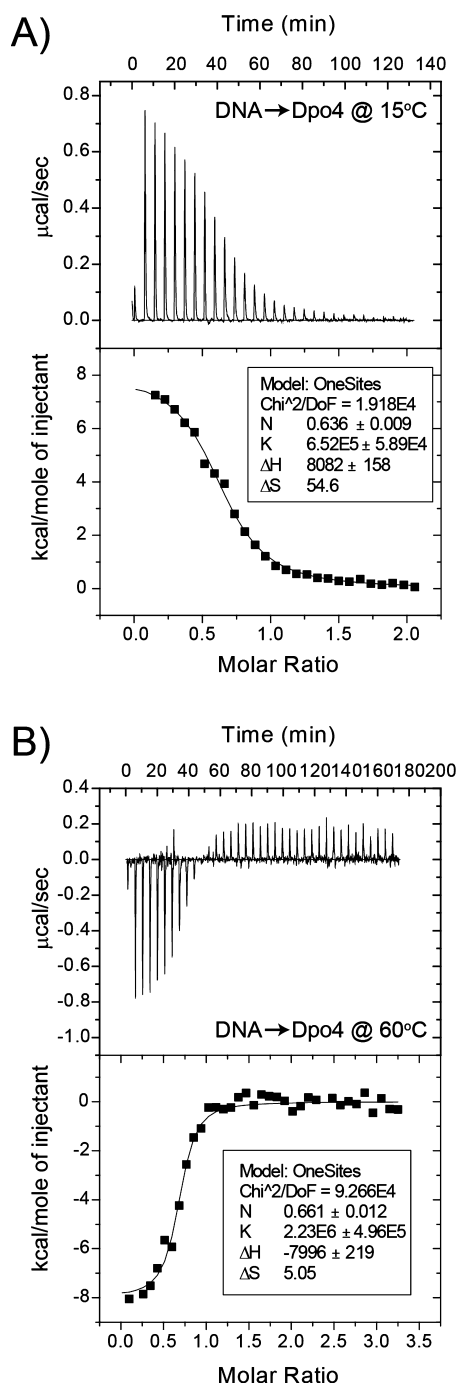


**Figure 2.** Stoichiometry and thermodynamics of binding of Dpo4 to DNA. ITC titration of 400  $\mu\text{M}$  DNA hairpin into 25  $\mu\text{M}$  *Sso*Dpo4 at (A) 15 and (B) 60  $^{\circ}\text{C}$  as described in Experimental Procedures. Data were fit using eq 1 to yield stoichiometries ( $n$ ) of  $0.64 \pm 0.01$  and  $0.66 \pm 0.01$  (DNA:Dpo4), apparent equilibrium association constants ( $K_{\text{app}}$ )  $(6.5 \pm 0.6) \times 10^5$  and  $(2.2 \pm 0.5) \times 10^6$  M, enthalpy changes ( $\Delta H^{\circ}_{\text{ITC}}$ ) of  $8.1 \pm 0.2$  and  $8.00 \pm 0.22$  kcal mol $^{-1}$ , and entropy changes ( $\Delta S^{\circ}_{\text{ITC}}$ ) of  $54.6$  and  $5.1$  cal mol $^{-1}$  K $^{-1}$  at 15 and 60  $^{\circ}\text{C}$ , respectively.

the binding is primarily enthalpically driven, and a fit of the binding isotherm to eq 1 gave the following values:  $K_{\text{app}} = (2.2 \pm 0.5) \times 10^6$  M $^{-1}$ ,  $\Delta H^{\circ}_{\text{ITC}} = -8.0 \pm 0.5$  kcal mol $^{-1}$ , and  $n = 0.66 \pm 0.01$ . The resulting  $\Delta G^{\circ}_{\text{ITC}}$  is  $-9.7$  kcal mol $^{-1}$ , and the calculated  $T\Delta S_{\text{ITC}}$  is  $1.7$  kcal mol $^{-1}$ . Importantly, the stoichiometries at 15 and 60  $^{\circ}\text{C}$  are similar and are consistent

with more than one molecule of Dpo4 bound to DNA. A dimer was also seen using chemical cross-linking. Although the titrations appear to go to completion, the stoichiometries do not saturate to  $n = 0.5$  (two Dpo4 molecules per DNA), indicating that the dimeric Dpo4 complex is in equilibrium with the monomer–DNA complex under these conditions.

**Analytical Velocity Sedimentation Detects the Formation of Oligomeric Dpo1 and Dpo4 Complexes with DNA.** Analytical ultracentrifugation (AUC) sedimentation velocity experiments were performed with either protein alone (Dpo1 or Dpo4) at 10, 20, or 30  $^{\circ}\text{C}$  to monitor the concentration and any temperature-dependent equilibria. For either Dpo1 or Dpo4 alone, there was an increase in the peak position of the sedimentation reaction boundary,  $ls\text{-}g^*(s)$ , with concentration (1 or 10  $\mu\text{M}$ ), as expected at each temperature based on 280 nm detection (Figure S1 of the Supporting Information). The sedimentation reaction boundaries were corrected for changes in the diffusion coefficient with temperature to give the sedimentation coefficient,  $s_{20,w}$ , and represent solution equilibrium distribution values for each experimental condition. Increasing the concentration of Dpo4 from 1 to 10  $\mu\text{M}$  did not change the  $s_{20,w}$  values significantly. At constant concentrations of Dpo1 or Dpo4, the weight average  $s_{20,w}$  value shifts to slightly higher values with an increase in temperature (Figure S1 of the Supporting Information). Analysis of the reaction boundaries for 10  $\mu\text{M}$  Dpo1 resulted in weight average  $s_{20,w}$  distribution values of  $4.19 \pm 0.01$ ,  $4.29 \pm 0.01$ , and  $4.32 \pm 0.01$  for 10, 20, and 30  $^{\circ}\text{C}$ , respectively. Similarly, analysis of the reaction boundaries for 10  $\mu\text{M}$  Dpo4 resulted in weight average  $s_{20,w}$  distribution values of  $2.52 \pm 0.01$ ,  $2.55 \pm 0.01$ , and  $2.59 \pm 0.01$  for 10, 20, and 30  $^{\circ}\text{C}$ , respectively. Increasing  $s_{20,w}$  values are consistent with a shift in the equilibrium toward the formation of larger species. For the protein alone (Dpo1 or Dpo4), these changes in  $s_{20,w}$  are only slightly significant over this limited temperature range.

More specific information about complex assembly can be obtained by examining the reaction boundaries for titration of each polymerase with a constant concentration (50 nM) of fluorescent hairpin primer–template DNA using analytical ultracentrifugation fluorescence-detected sedimentation (AU-FDS).<sup>48</sup> By monitoring the reaction boundaries of fluorescent DNA in the AUC velocity experiments, we are able to examine a much greater dynamic range of protein concentrations (50–5000 nM) than with absorbance alone. Titration of Dpo1 at 10, 20, and 30  $^{\circ}\text{C}$  shows a clear increase in the  $s_{20,w}$  distributions and boundaries with concentration, consistent with the detection of multiple protein-bound DNA complexes (Figure 3A–C). Here, discrete  $s_{20,w}$  populations for monomeric and trimeric Dpo1 can be identified. Interestingly, the  $s_{20,w}$  reaction boundaries at identical concentrations of Dpo1 bound to DNA shift toward larger species with an increase in temperature more significantly than for the free protein alone. For example, via the specific examination of 100 nM Dpo1 across the three temperatures, the weight average  $s_{20,w}$  values increase with increasing temperature:  $4.66 \pm 0.03$ ,  $4.77 \pm 0.01$ , and  $4.86 \pm 0.01$  at 10, 20, and 30  $^{\circ}\text{C}$ , respectively (Figure S2A of the Supporting Information). At 1  $\mu\text{M}$  Dpo1, the weight average  $s_{20,w}$  values increase to  $5.71 \pm 0.01$ ,  $5.89 \pm 0.01$ , and  $6.04 \pm 0.01$ , respectively (Figure S2B of the Supporting Information).

Titration of Dpo4 on fluorescent hairpin primer–template DNA using AU-FDS also shows an increase in the  $s_{20,w}$  boundaries at each temperature (Figure 3D–F), consistent with populations consisting of both monomeric and dimeric

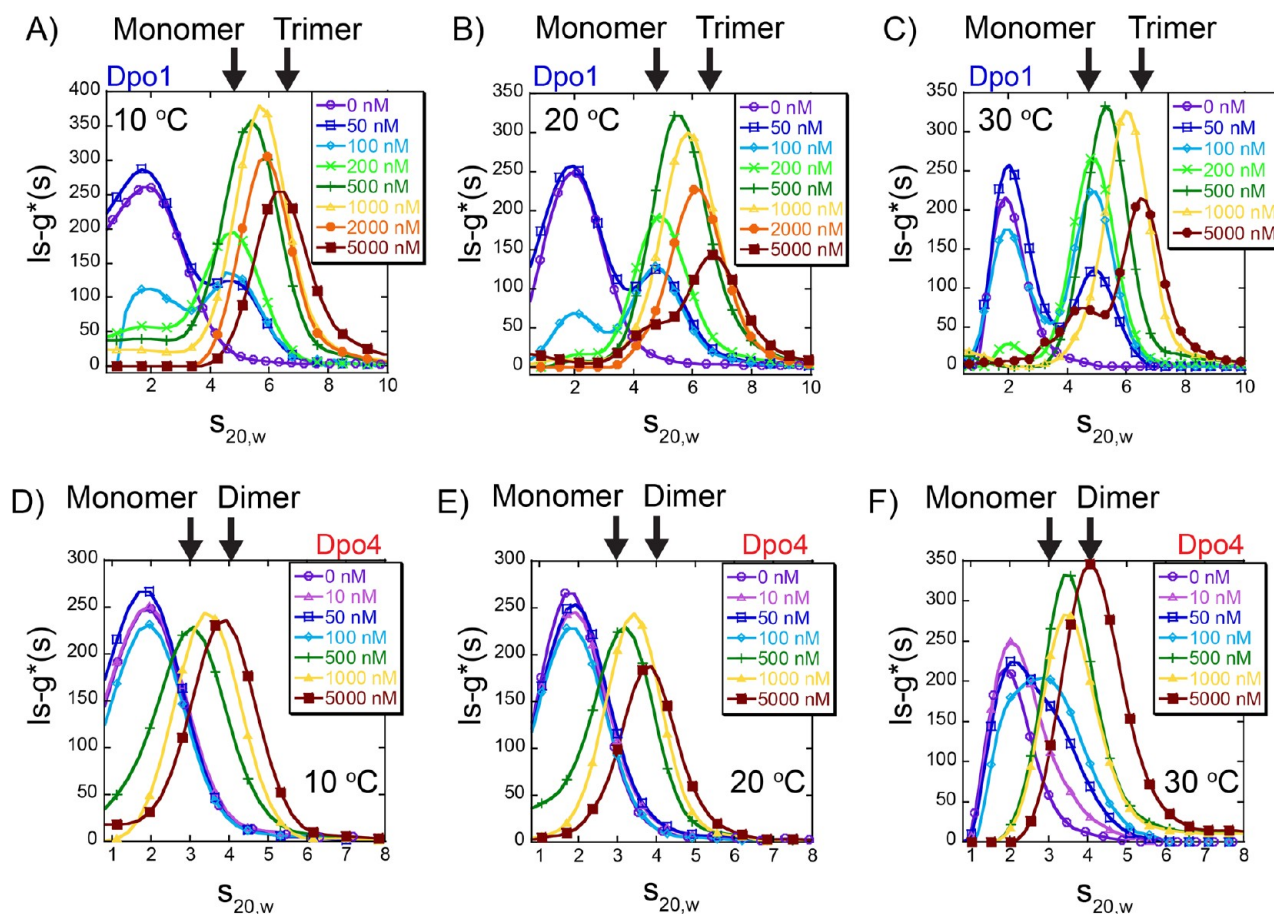


**Figure 3.** Solution assembly of oligomeric polymerases on DNA. Analytical ultracentrifugation velocity fluorescence-detected sedimentation (AU-FDS) experiments showing the  $ls-g^*(s)$  distribution profiles as a function of Dpo1 or Dpo4 concentration: 0 (○, purple), 10 (△, pink), 50 (□, blue), 100 (◇, cyan), 200 (×, light green), 500 (+, dark green), 1000 (▲, yellow), 2000 (●, orange) and 5000 nM (■, brown) at (A and D) 10 °C, (B and E) 20 °C, or (C and F) 30 °C. Every fifth data point is indicated for the sake of simplicity, and all data were fit as described in Experimental Procedures.  $s_{20,w}$  positions representing monomer or trimer Dpo1 and monomer or dimer Dpo4 are indicated by arrows.

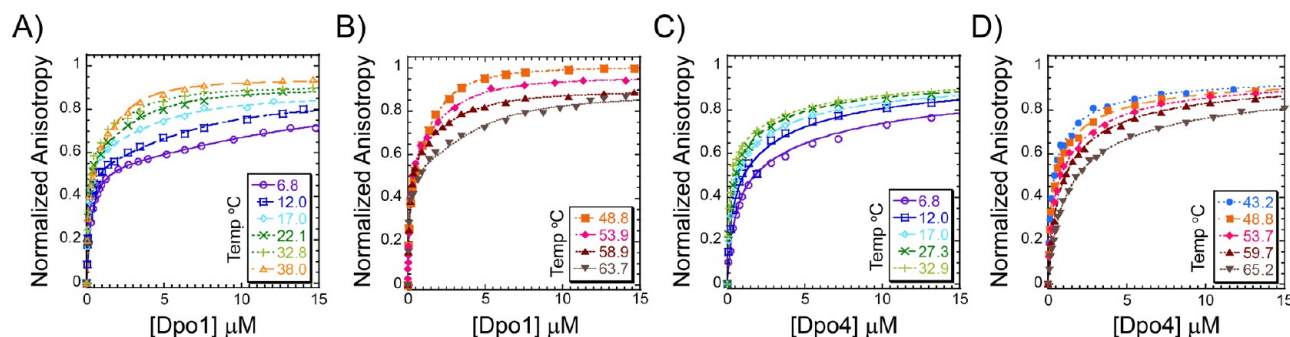


**Figure 4.** Quantification of individual binding steps leading to oligomeric polymerase–DNA complexes. Representative normalized individual equilibrium fluorescence anisotropy titrations for (A and B) Dpo1 and (C and D) Dpo4 binding to DNA at low or high temperatures. Data are included for both lower [6.8 (○, purple), 12.0 (□, blue), 17.0 (◇, cyan), 22.1 or 27.3 (×, dark green), 32.8 or 32.9 (+, light green), and 38.0 (△, light orange)] and higher [43.2 (●, blue), 48.8 (■, dark orange), 53.7 or 53.9 (◆, pink), 58.9 or 59.7 (▲, brown), and 63.7 or 65.7 °C (▼, gray)] temperatures. The individual data points were fit to eq 5 to determine  $K_{d1}$  and  $K_{d2}$  values for Dpo4 or Dpo1. At least three independent titrations were performed and fit at each temperature, and the resulting values are listed in Table 1.

Dpo4–DNA complexes. Binding of Dpo4 to DNA does not appear to occur until the Dpo4 concentration exceeds 100 nM at 10, 20, or 30 °C. Moreover, the reaction boundary continually shifts to larger species between 500 and 5000 nM. Similar to the behavior of Dpo1, the reaction boundaries at constant concentrations of Dpo4 measured at 10, 20, and 30 °C also increase or shift to slightly larger weight average complexes

more significantly than protein alone. Examination of 5  $\mu\text{M}$  Dpo4 at the three temperatures (10, 20, and 30 °C) shows that the weight average  $s_{20,w}$  values are  $3.79 \pm 0.02$ ,  $3.84 \pm 0.01$ , and  $4.12 \pm 0.01$ , respectively (Figure S2D of the Supporting Information). The equilibrium shift in the sedimentation coefficients with temperature can be most clearly seen at 100 nM Dpo4 (Figure S2C of the Supporting Information) where



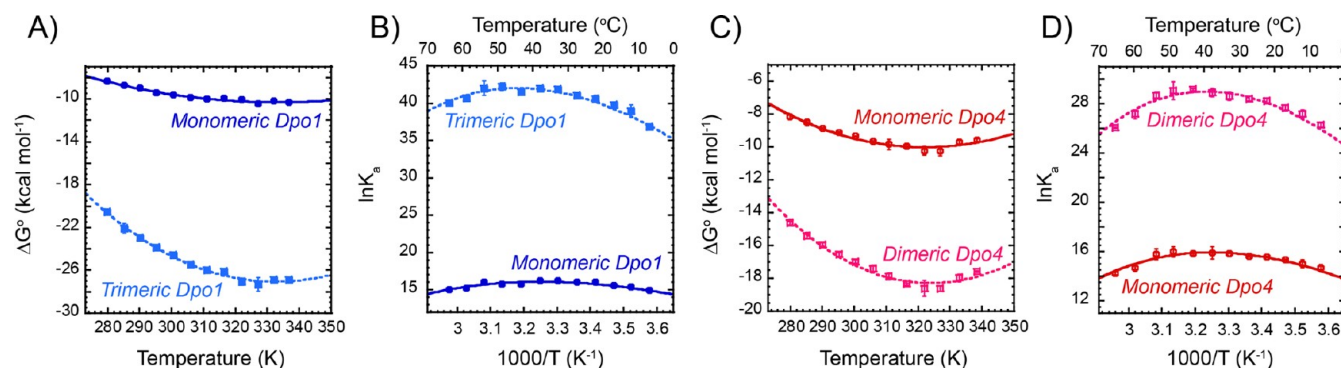


**Figure 5.** Thermodynamic differences between monomeric and oligomeric Dpo1 and Dpo4 binding to DNA. Gibbs–Helmholtz plots of the free energy of binding ( $\Delta G^\circ$ ) for (A) monomeric (solid line, ●, blue) or trimeric (dashed line, ■, light blue) Dpo1 and (C) monomeric (solid line, ○, red) or dimeric (dashed line, □, pink) Dpo4 as a function of temperature. Error bars represent the standard error from multiple experiments at each point. Lines show the fits of the data to eq 8 giving  $\Delta C_p^\circ$  values for monomeric ( $-0.43 \pm 0.07 \text{ kcal mol}^{-1} \text{ K}^{-1}$ ) and trimeric ( $-1.45 \pm 0.14 \text{ kcal mol}^{-1} \text{ K}^{-1}$ ) Dpo1 and monomeric ( $-0.68 \pm 0.10 \text{ kcal mol}^{-1} \text{ K}^{-1}$ ) and dimeric ( $-1.22 \pm 0.15 \text{ kcal mol}^{-1} \text{ K}^{-1}$ ) Dpo4. van't Hoff plots highlighting the individual binding states for (B) Dpo1 and (D) Dpo4. Lines show the fits to eq 11.

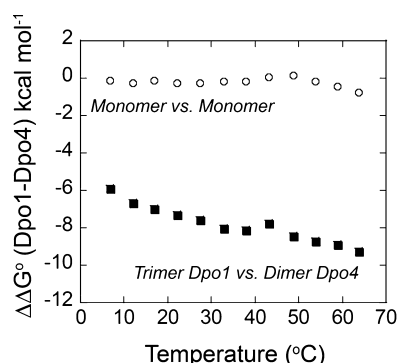


**Figure 6.** Gibbs free energy differences ( $\Delta\Delta G^\circ$ ) for DNA binding, comparing Dpo1 to Dpo4 monomers (○) or comparing trimeric Dpo1 to dimeric Dpo4 (■), plotted as a function of temperature.

initial binding is observed at only 30 °C. This observation agrees well with the fluorescence anisotropy data below which a  $K_{d1}$  value of  $0.130 \pm 0.004 \mu\text{M}$  is measured at 33 °C, but larger  $K_{d1}$  values are seen at lower temperatures (Table 1).

**Temperature-Dependent Separation of Polymerase Binding Events Using Fluorescence Anisotropy.** To investigate further the individual binding events of Dpo1 or Dpo4 on DNA, we used fluorescence anisotropy to evaluate the

**Table 1. Equilibrium Fluorescence Anisotropy Binding Parameters for Polymerase Binding to DNA**

Dpo1			Dpo4		
temp (°C)	$K_{d1} (\mu\text{M})^a$	$K_{d2} (\mu\text{M})^a$	temp (°C)	$K_{d1} (\mu\text{M})^a$	$K_{d2} (\mu\text{M})^a$
6.8	$0.32 \pm 0.02$	$17 \pm 0^b$	6.8	$0.44 \pm 0.12$	$9.3 \pm 0.9$
12.0	$0.21 \pm 0.06$	$8.0 \pm 1.2$	12.0	$0.33 \pm 0.11$	$5.2 \pm 0.1$
17.0	$0.17 \pm 0.02$	$5.8 \pm 0.1$	17.0	$0.21 \pm 0.00$	$4.7 \pm 1.0$
22.2	$0.11 \pm 0.02$	$4.7 \pm 0.8$	22.1	$0.18 \pm 0.01$	$3.2 \pm 0.7$
27.4	$0.11 \pm 0.00^b$	$3.7 \pm 0.3$	27.3	$0.16 \pm 0.01$	$2.8 \pm 0.4$
32.8	$0.09 \pm 0.00^b$	$2.7 \pm 0.1$	32.9	$0.13 \pm 0.00^b$	$3.0 \pm 0.9$
38.0	$0.10 \pm 0.00^b$	$2.5 \pm 0.1$	37.8	$0.14 \pm 0.07$	$2.3 \pm 0.4$
43.3	$0.14 \pm 0.00^b$	$2.6 \pm 0.2$	43.2	$0.13 \pm 0.03$	$1.7 \pm 0.5$
48.8	$0.14 \pm 0.02$	$1.8 \pm 0.4$	48.8	$0.13 \pm 0.05$	$2.3 \pm 0.9$
53.9	$0.11 \pm 0.03$	$2.4 \pm 0.8$	53.8	$0.15 \pm 0.07$	$2.7 \pm 1.0$
58.9	$0.21 \pm 0.02$	$3.2 \pm 0.2$	58.9	$0.44 \pm 0.12$	$3.8 \pm 0.3$
63.7	$0.20 \pm 0.03$	$4.5 \pm 0.4$	65.2	$0.67 \pm 0.08$	$7.2 \pm 0.9$

<sup>a</sup> $K_{d1}$  and  $K_{d2}$  are the equilibrium dissociation constants for the first and second binding events, respectively. Values are means and standard errors from parameters fit to eq 5 from at least three independent titration experiments at each temperature. <sup>b</sup>Standard error <0.005.

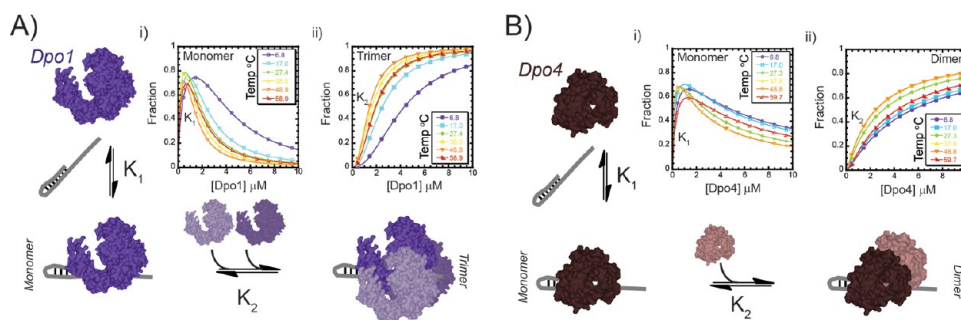


**Figure 7.** Concentration-dependent assembly of oligomeric polymerase–DNA complexes. (A) Trimeric Dpo1 assembly on DNA follows the initial higher-affinity binding of one molecule ( $K_1$ ) followed by a second step of cooperative assembly of two additional molecules ( $K_2$ ). (B) Assembly of dimeric Dpo4 on DNA that includes two sequential binding events with differing affinities ( $K_1$  and  $K_2$ ). Simulations of the relative populations for monomeric (i) Dpo1 or Dpo4 (empty symbols, representing  $K_1$ ) or (ii) trimeric Dpo1 or dimeric Dpo4 (filled symbols, representing  $K_2$ ) as a function of temperature and concentrations as described in the Supporting Information. Simulations are shown for temperatures of 6.8 (purple ○ or ●), 17.0 (cyan □ or ■), 27.4 (green ◇ or ◆), 38.0 (yellow △ or ▲), 48.8 (orange ▽ or ▼), and 58.9 or 59.7 °C (red □ or right triangles).

constants for the monomeric ( $K_{d1}$ ) and subsequent oligomeric ( $K_{d2}$ ) binding steps over a range of temperatures. The melting temperature ( $T_M$ ) of the DNA primer–template hairpin was measured from a shift in the UV absorbance and found to be 88 °C (data not shown), which is well above our experimental temperature range. Protein was titrated into low concentrations of a Cy3-labeled DNA primer–template hairpin, and the increase in fluorescence anisotropy due to binding was monitored (Figure 4). The increase in anisotropy as a function of Dpo1 concentration was fit to either a single-binding site model (eq 4) or a sequential-binding site model (eq 5) (Figure 4A,B and Figure S3A of the Supporting Information). The second and third individual binding events for Dpo1 cannot be separated from our EMSA or ITC data (ref 20 and manuscript in preparation); therefore, simultaneous or cooperative binding is hypothesized. The increase in anisotropy as a function of Dpo4 concentration was also fit to either eq 4 or 5. Equation 5 provided the best fit of the data for Dpo4 (Figure 4C,D and Figure S3B of the Supporting Information). The fits of these individual equations to the data are consistent with stoichiometric values and processes measured by ITC, chemical cross-linking, AUC, EMSA, and gel filtration.<sup>20</sup> The differences in the individual  $K_d$  values ( $K_{d1}$  and  $K_{d2}$ ) for each DNA polymerase are greater than 10-fold (Table 1) and generally decrease concurrently with temperature up to 50 °C.  $K_{d2}$ , fit from the anisotropy experiments, is the intrinsic constant for binding of one of the two monomers in the second step, while  $K_{d2}^2$  represents the constant for simultaneous binding of both Dpo1 monomers in the second “step” to form the trimeric Dpo1–DNA complex.

The temperature dependencies of the monomeric and trimeric binding equilibria of Dpo1 and DNA are plotted in a Gibbs–Helmholtz plot ( $\Delta G^\circ$  vs  $T$ ) (Figure 5A) or a van’t Hoff plot ( $\ln K$  vs  $1000/T$ ) (Figure 5B) and reported in Table S1 of the Supporting Information. Analysis by these two methods allows for easy visualization of any nonlinearity in the temperature dependence of binding for each molecular event. The overall free energy for trimeric Dpo1 binding to DNA is the sum of the free energies for the first and second binding steps, where the second step represents the simultaneous or cooperative binding of two additional monomers to the monomeric Dpo1–DNA complex (described in Table 2).

**Table 2. Definition of Equilibrium Steps and Polymerase States**

step <sup>a</sup>	Dpo1		Dpo4	
	$K_{app}$	$\Delta C_p^{(app)} (kcal\ mol^{-1}\ K^{-1})$	$K_{app}$	$\Delta C_p^{(app)} (kcal\ mol^{-1}\ K^{-1})$
first	$K_1$	−0.43	$K_1$	−0.68
second	$K_2^2$	−1.02	$K_2$	−0.51
overall <sup>b</sup>	$K_1(K_2)^2$	−1.45	$K_1K_2$	−1.22

<sup>a</sup>As measured from fluorescence anisotropy. <sup>b</sup>Product of equilibrium constants leading to trimeric Dpo1 or dimeric Dpo4.

Notably, monomeric Dpo1 has a relatively small binding advantage over monomeric Dpo4, compared with a much larger difference in free energy of binding for trimeric Dpo1 over dimeric Dpo4 (Figure 6). The free energy minima for monomeric and trimeric Dpo1 binding both occur at ~61 °C. The predicted critical temperatures for  $T_H$  (where  $\Delta H = 0$ ) and  $T_S$  (where  $T\Delta S = 0$ ) are 36 and 60 °C for monomeric and 41 and 60 °C for trimeric Dpo1, respectively.  $T_H$  represents the

temperature at which  $K_a$  is maximal, and  $T_S$  represents the temperature at which  $\Delta G$  is most favorable. This binding behavior is indicative of temperature-dependent binding enthalpies ( $\Delta H^\circ$ ) with fitted heat capacity changes ( $\Delta C_p^\circ$ ) (eq 8) for monomeric and trimeric Dpo1 binding equal to  $-0.43 \pm 0.07$  and  $-1.02 \pm 0.12\ kcal\ mol^{-1}\ K^{-1}$ , respectively (Table S1 of the Supporting Information). The parallel large decreases in  $\Delta H^\circ$  and  $T\Delta S^\circ$  with temperature are compensatory, resulting in smaller changes in  $\Delta G^\circ$ , and are generally characteristic of sequence-specific DNA binding proteins (Figure S4A,B of the Supporting Information).<sup>29,30,49</sup> It seems possible that Dpo1 and the DNA at the primer–template junction achieve a degree of structural complementarity comparable to that in sequence-specific protein–DNA interfaces, thus making a significant contribution to the large negative  $\Delta C_p^\circ$ . Subsequent structure-specific binding of two additional molecules of Dpo1 at that site completes the trimeric Dpo1–DNA complex as identified previously by DNA footprinting.<sup>20</sup>

Dpo4 also shows a nonlinear temperature dependence of binding for both the monomer and dimer, as visualized in a Gibbs–Helmholtz plot (Figure 5C) or van’t Hoff plot (Figure 5D) and reported in Table S2 of the Supporting Information. The free energy minima for monomeric and dimeric Dpo4 assemblies occur at ~49 and 51 °C, respectively. The predicted critical temperatures for  $T_H$  and  $T_S$  are 34 and 49 °C for monomeric and 39 and 55 °C for dimeric Dpo4, respectively. The temperature at which Dpo4 binding shifts from primarily entropically driven to enthalpically driven occurs in the range of 35–40 °C and is consistent with the ITC results from Figure 2. This binding behavior is also indicative of a temperature-dependent  $\Delta H^\circ$  with fitted  $\Delta C_p^\circ$  values (eq 8) for monomeric and dimeric Dpo4 binding of  $-0.68 \pm 0.09$  and  $-1.22 \pm 0.15\ kcal\ mol^{-1}\ K^{-1}$ , respectively. Again, parallel changes in  $\Delta H$  and  $T\Delta S$  with temperature are indicative of temperature-dependent enthalpy–entropy compensation (Figure S4C,D of the Supporting Information).

**Calculated  $\Delta C_p$  Values from the Burial of Nonpolar and Polar Surfaces upon Formation of the Dpo4–DNA Complex.** The burial of polar and nonpolar surface areas upon binding has been used as a predictive measure relating structural details to thermodynamic parameters. Heat capacity data for the transfer of small molecule model hydrocarbons and amides from the liquid state to the aqueous solution were used to obtain an empirical relationship for the calculation of  $\Delta C_p^{ASA}$  (see eq 12) from computed values of changes in nonpolar and polar surfaces upon protein folding or protein–ligand interaction.<sup>46,50</sup> For the folding of many proteins and the interaction of proteins with small ligands, there has been adequate agreement between the experimentally observed  $\Delta C_p$  values and those predicted from the burial of surface area. However, for association of macromolecules and some protein folding reactions, there are many additional solution factors that contribute to the strongly negative observed  $\Delta C_p$  values. A significant source of the discrepancy between  $\Delta C_p^{obs}$  and  $\Delta C_p^{ASA}$  values is the restriction of configurational (conformational–vibrational) degrees of freedom upon association.<sup>35,51–55</sup>

Although the buried surface area for Dpo1 binding to DNA cannot be determined directly because of the lack of an appropriate crystal structure, 3437 Å<sup>2</sup> of surface area is buried when a Dpo4 monomer binds to primer–template DNA.<sup>44</sup> The changes in polar ( $\Delta A_p$ ) and nonpolar ( $\Delta A_{np}$ ) solvent accessible surface area upon Dpo4 binding to DNA are −1753 and −1683



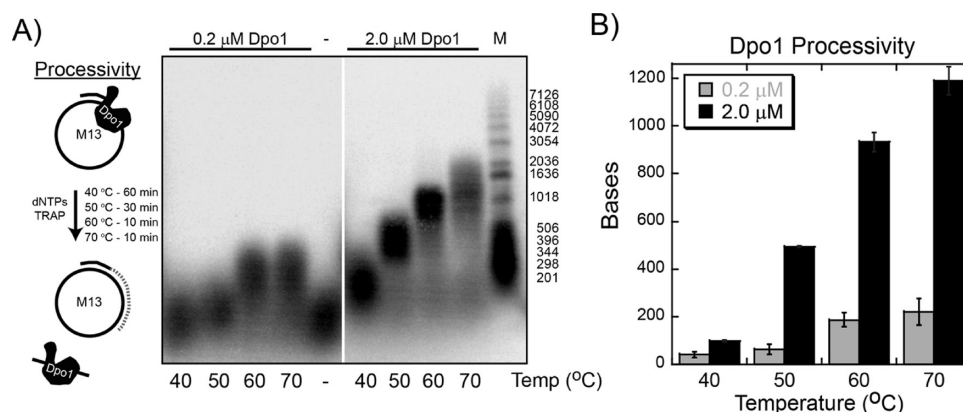


**Figure 8.** Processivity of Dpo1 increases with temperature and concentration. (A) Dpo1 processivity assays were performed at 40, 50, 60, and 70 °C representing monomer (0.2  $\mu$ M) (left) or trimer (2.0  $\mu$ M) (right) concentrations and separated on a denaturing alkaline agarose gel as described in Experimental Procedures. The inset cartoon describes the experimental protocol for processivity experiments. Longer reaction times were used for lower temperatures to compensate for slower polymerase rates. Processivity values were calculated from DNA size markers and calculated using ImageQuant. (B) Quantification of the processivity values (base pairs) comparing monomeric (200 nM, gray) or trimeric (2.0  $\mu$ M, black) Dpo1 at 40, 50, 60, and 70 °C.

$\text{\AA}^2$ , respectively. From these values, we calculate a  $\Delta C_p^{\text{ASA}}$  value of  $-0.29 \text{ kcal mol}^{-1} \text{ K}^{-1}$  at 25 °C for monomeric Dpo4 binding to DNA from surface area contributions alone. As noted above, although the burial of nonpolar ( $\Delta A_{\text{np}}$ ) or polar ( $\Delta A_{\text{p}}$ ) surface areas is often considered the most important factor contributing to  $\Delta C_p^\circ$ , other factors such as electrostatics, solvation, protonation, conformational strain, thermal or vibrational fluctuations, and linked equilibria can often make much larger contributions to  $\Delta C_p^\circ$  accounting for deviation from the experimental value (Figure 6).<sup>56</sup>

**Modeling Temperature-Dependent Binding Populations of Dpo1 and Dpo4.** Using a sequential assembly scheme with a cooperativity parameter for Dpo1 or with no cooperativity parameter for Dpo4, and the parameters from the anisotropy experiments, we are able to model the relative populations of the monomer or oligomer of Dpo1 or Dpo4 bound to DNA as a function of temperature (Figure 7 and Supporting Information). Using this analysis, there is both a concentration- and temperature-dependent effect on the formation of monomeric or oligomeric Dpo1 or Dpo4. Below 400 nM, there is preferential binding of monomeric Dpo1 and Dpo4 to DNA. In the range between 400 and 2000 nM, there is a mixed population of complexes of monomeric and oligomeric Dpo1 or Dpo4 with DNA. At concentrations of  $>2 \mu\text{M}$ , there is preferential binding of trimeric Dpo1 and dimeric Dpo4. In this analysis, it is also clear that the assemblies and populations are influenced by temperature. For Dpo1, there is an increase in affinity for both the first and second binding events up to 50 °C. Above 50 °C, there is a slight decrease in the second binding step in favor of the first. A similar trend occurs for Dpo4 with the cutoff being around 45 °C. More than 50% of the Dpo1 population exists in a trimeric state at concentrations of  $>1.5 \mu\text{M}$ , while a Dpo4 concentration of 3  $\mu\text{M}$  is required for 50% dimer.

**Dpo1 and Dpo4 Processivities Increase with Temperature and Concentration.** To provide a biochemical explanation for the different binding specificities for DNA polymerases across a variety of temperatures, we assayed the temperature-dependent polymerization processivity for Dpo1 and Dpo4. Processivity is a measure of the stability of an enzyme–substrate complex during successive catalytic steps. Processive DNA polymerases have a higher rate constant for

the catalytic step of DNA synthesis ( $k_{\text{pol}}$ ) than for dissociation from the template ( $k_{\text{dis}}$ ).<sup>57</sup> The ratio between these kinetic parameters determines the processivity value. The processivity for Dpo4 has been measured previously over a limited concentration range of 0.5–200 nM representing primarily monomer, and although there is a slight increase in processivity with concentration, it was concluded that Dpo4 is essentially a distributive enzyme with processivity value of one to two nucleotides.<sup>17</sup> Interestingly, in processivity reactions where the concentration of Dpo4 was 20-fold greater than the DNA concentration, products  $>100$  nucleotides in length were synthesized, suggesting that polymerase interactions may modestly increase processivity. Another report of processivity when the DNA template was in excess of Dpo4 (35 nM) gave a value of 16 at 37 °C.<sup>23</sup> More strikingly, we have previously measured a large increase in processivity for Dpo1 when it is in the trimeric conformation over that of the monomeric form.<sup>20</sup>

We have performed additional DNA polymerization experiments at various temperatures (40, 50, 60, and 70 °C) to determine if higher temperatures promote greater rates or processivities for Dpo1 because of increased binding specificity. Both kinetic and processivity experiments were performed at either 200 nM or 2.0  $\mu\text{M}$  Dpo1 to represent contributions from primarily monomeric or trimeric species, respectively (Figure 8A). We chose 40 °C over room temperature experiments because of the slower rates of synthesis that would limit detection. The DNA synthesis rates for trimeric Dpo1 at 40, 50, 60, and 70 °C were measured to be  $36 \pm 3$ ,  $209 \pm 4$ ,  $447 \pm 30$ , and  $529 \pm 35$  bp/min, respectively, and always greater than the monomeric Dpo1 rates of  $36 \pm 12$ ,  $76 \pm 14$ ,  $366 \pm 45$ , and  $400 \pm 55$  bp/min, respectively (Figure S6 of the Supporting Information). Processivity experiments were initiated with the simultaneous addition of dNTPs and a high concentration of unlabeled DNA trap. Polymerase molecules that dissociate from the prebound radioactive primer-M13 template will be captured by binding to a cold DNA substrate and no longer contribute to the signal for the experiment. The concentration of trap required to be effective at all polymerase concentrations was determined empirically by titrating trap until no further increase in processivity was noted (data not shown). Reaction mixtures were incubated for different times at each temperature depending on the rate of synthesis. Dpo1 processivity at 200

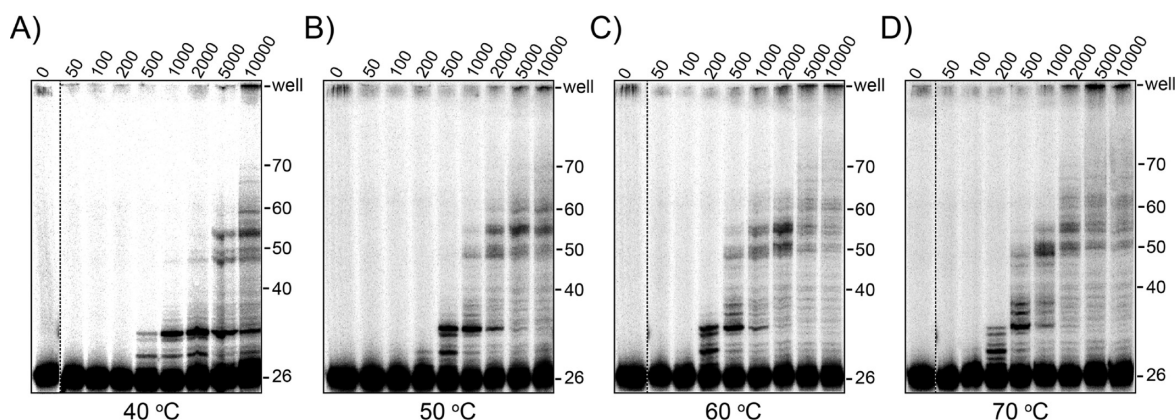


**Figure 9.** Processivity of Dpo4 increases with temperature and concentration. Dpo4 processivity assays were performed at (A) 40, (B) 50, (C) 60, and (D) 70 °C for concentrations ranging from 0.05 to 10  $\mu$ M and separated on a denaturing acrylamide gel. Reactions were initiated with dNTPs and excess ssDNA trap as described in Experimental Procedures.

nM (representing monomer) increased slightly with an increase in temperature to  $41 \pm 12$ ,  $62 \pm 14$ ,  $187 \pm 45$ , and  $220 \pm 56$  nucleotides at 40, 50, 60, and 70 °C, respectively (Figure 8B). The processivity at 2  $\mu$ M (representing trimer) increased more dramatically to  $98 \pm 2$ ,  $493 \pm 5$ ,  $933 \pm 39$ , and  $1191 \pm 52$  nucleotides at 40, 50, 60, and 70 °C, respectively (Figure 8B). At  $\geq 50$  °C, the processivity of the trimeric state of Dpo1 is much greater than that of the monomeric complex and reflects a change in the specificity of binding DNA consistent with the fluorescence anisotropy data presented above.

For Dpo4, processivities also increase with an increase in enzyme concentration at a variety of temperatures (Figure 9) but to a lesser extent than for Dpo1. As for Dpo1, the Dpo4 processivity increases slightly at 200 nM (representing monomer) and more dramatically at 5  $\mu$ M (representing dimer) with an increase in temperature (Figure S7 of the Supporting Information). This is visualized not only by longer products separated on the gel but also by more radioactivity seen in the wells at the higher concentrations or temperatures. Interestingly, at both monomeric and dimeric Dpo4 concentrations, there is an apparent decrease in processivity upon going from 60 to 70 °C, consistent with the decreased specificity of binding measured for Dpo4 at those temperatures using fluorescence anisotropy (Figure 5C). Similar to those of Dpo1, the processivity values increase when dimeric Dpo4 concentrations are used compared with monomeric Dpo4 concentrations at all temperatures.

## DISCUSSION

Using chemical cross-linking, isothermal titration calorimetry, analytical ultracentrifugation, and fluorescence anisotropy, we have been able to identify, separate, and quantify multiple binding events for DNA replication (Dpo1) and repair polymerases (Dpo4) with DNA that lead to different specificities and activities with temperature. Consistent with our previous report,<sup>20</sup> Dpo1 forms a concentration-dependent trimer at all temperatures. Unexpectedly, Dpo4 behaves similarly, forming a dimeric complex that becomes more favored at higher temperatures. For both Dpo1 and Dpo4, the affinities of monomeric and subsequent oligomeric binding generally increase as the temperature approaches the physiological range. The changes in polymerase equilibria with concentration and temperature can be clearly visualized using analytical ultracentrifugation even over a limited temper-

ature range (10–30 °C). Comparison of monomeric polymerase binding to DNA shows that the differentially stronger affinity of Dpo1 than Dpo4 becomes even more exaggerated as physiological temperatures (75 °C) are approached, providing for thermodynamic selection of a DNA replication polymerase on undamaged templates. These thermodynamic results are reflected in the enzymatic behaviors, in that we measured a greater processivity for nucleotide incorporation at higher temperatures and oligomeric states for both DNA polymerases. The equilibrium microenvironment in the cell or more importantly at the replication fork will direct binding and association of a variety of DNA polymerase complexes to promote efficient DNA replication in the presence of any damage.

**Evidence of Oligomeric Dpo1 and Dpo4 Complexes Bound to DNA.** Identification, isolation, and assembly of the trimeric Dpo1 complex at the primer–template junction have been discussed previously<sup>20</sup> but have now been verified and quantified across a large temperature range. Similarly, cross-linking and ITC suggest that assembly of a dimeric Dpo4 is also possible. Using AU-FDS experiments, we were able to directly monitor the size distribution of polymerase DNA complexes in solution at multiple temperatures. Interestingly, for both Dpo1 and Dpo4 bound to DNA, there is a modest but reproducible shift in the sedimentation boundaries to larger coefficients with an increase in temperature. Unfortunately, analytical ultracentrifugation can be performed only over a limited temperature range, 10–30 °C, as these effects may have been stronger if higher temperatures could have been probed. A shift to a larger  $s_{20,w}$  value in sedimentation velocity experiments is consistent with a change in the population of complexes toward a larger average size. The shifts in reaction boundaries occur at lower concentrations for Dpo1 than for Dpo4, consistent with the anisotropy result that Dpo1 has a higher affinity for DNA than Dpo4 at identical temperatures. Distinct  $s_{20,w}$  populations are more easily seen for Dpo1, because of large differences in the molecular weight between the complexes of the monomer and trimer with DNA. For Dpo4, the size difference between monomeric and dimeric bound states is much smaller, causing a general broadening of the  $s_{20,w}$  distribution, and discrete  $s_{20,w}$  weight average values for each state are not observed. The most obvious temperature-dependent reaction boundary shifts occur at concentrations equal to the dissociation constant for polymerase binding to DNA (i.e., 100 nM Dpo4 at 30 °C in

Figure S2C of the Supporting Information). Shifts in the reaction boundaries of Dpo1 bound to DNA with an increase in temperature are more subtle, but reproducible, in this experimental range; these shifts are characterized by a better resolution between monomeric and trimeric Dpo1 at 30 °C (Figure 3C). Although only qualitatively, the individual sedimentation boundaries correlate well with the  $K_{d1}$  and  $K_{d2}$  binding affinities ( $K_1$  and  $K_2$  in Figure 7) for binding of Dpo1 and Dpo4 to DNA measured by fluorescence anisotropy. Sedimentation equilibrium experiments would be useful in quantifying the actual populations for either Dpo1 or Dpo4 alone or bound to DNA but unfortunately resulted in uninterpretable spectra, probably because of some precipitation or aggregation during the long times required to attain sedimentation equilibrium. No loss of spectral signal was detected in the analytical velocity experiments, suggesting that aggregation and precipitation are not issues for shorter time scales.

Although there are a number of biochemical, kinetic, and structural papers involving the mechanism of action for Dpo4,<sup>17,18,23,24,44,58–62</sup> none of them suggest that a dimeric DNA polymerase complex is the active species. However, we have confirmed Dpo4 binding to DNA as a dimer using chemical cross-linking, the stoichiometry values from ITC, and analytical ultracentrifugation. The apparent dissociation constants measured by ITC at 15 °C ( $K_d^{ITC} = 1.5 \mu\text{M}$ ) or 60 °C ( $K_d^{ITC} = 0.45 \mu\text{M}$ ) are much larger than expected based on AUC, fluorescence anisotropy, and EMSA results previously published<sup>63–65</sup> and most likely represent contributions of equilibria from monomer and dimer Dpo4 binding to DNA. The analytical ultracentrifugation results show that binding begins at a concentration of 100 nM and then proceeds in a concentration-dependent manner toward dimer above 500 nM. According to the fits of the fluorescence anisotropy experiments, dimer assembly persists across a range of temperatures. From a variety of Dpo4–DNA X-ray structures, the site size of Dpo4 on DNA consists of roughly 10 bases of dsDNA and 4 bases of ssDNA straddling the primer–template junction.<sup>18</sup> The DNA hairpin primer–template junction used in these studies has a 12 bp duplex and a 10 bp single-strand region, thus restricting binding site size to a single DNA polymerase. The location of the protein cross-link can be pinpointed because there is only a single native cysteine residue (C31) in Dpo4 but does not exclude other dimeric Dpo4 structures. Unlike what we observed for Dpo1,<sup>20</sup> the presence of DNA did not significantly affect the degree of cross-linking, suggesting that at the concentrations used for this experiment, Dpo4 can form a dimer in the absence of DNA.

Within the RCSB Protein Data Bank (<http://www.rcsb.org>), there exist roughly 100 structures of Dpo4 both without DNA and bound to various types of DNA templates (damaged and undamaged). Roughly one-third of these structures have multiple Dpo4 molecules interacting in the crystal unit in various conformations. Many of these multimeric structures show Dpo4 in a conformation that would allow the cysteine residues in the interface to be in sufficient proximity for cross-linking to occur.<sup>66–68</sup> The rest of the oligomeric Dpo4 structures are in a variety of alternative dimeric or tetrameric complexes. Additionally, a number of structures for the analogous Dbh polymerase from *Sulfolobus acidocaldarius* also show oligomeric complexes in the crystal unit with the homologous cysteine residue in sufficient proximity for cross-linking.<sup>69,70</sup> Although we cannot be certain of the exact

conformation, we are able to detect and verify a previously unrecognized dimeric Dpo4 complex across all temperature ranges that is consistent with our thermodynamic binding data. Moreover, the variety of dimeric and tetrameric states of Dpo4 seen by X-ray crystallography may suggest that the binding equilibria have even greater complexity than we include in our model (Figure 7B).

**Thermodynamic Differences in Binding Oligomeric Replication and Repair Polymerases to Primer–Template DNA.** In fluorescence anisotropy experiments, optimal fits to binding isotherms for the titration of Dpo1 or Dpo4 with DNA are obtained using a model for a sequential assembly path involving two binding events. Information from cross-linking, EMSA, gel filtration, AUC, and ITC<sup>20</sup> experiments about the initial (monomeric) and final (trimeric for Dpo1 and dimeric for Dpo4) forms of polymerase–DNA complexes was essential for differentiating between single and multiple binding events in the anisotropy experiments. For Dpo1 and Dpo4, there is an initial higher-affinity binding of one polymerase molecule to DNA. The binding of the second and third molecules of Dpo1 to complete the trimer is proposed to occur cooperatively,<sup>20</sup> however, because a dimeric Dpo1–DNA complex cannot be resolved, our data are insufficient to separate these secondary binding events. Formation of a Dpo4 dimer proceeds through two sequential binding events. For both Dpo1 and Dpo4, binding of additional polymerase molecule(s) to the first is inferred primarily from the limited DNA template size and the direct contacts found using chemical cross-linking.<sup>20</sup> Previous reports of binding affinity for Dpo1<sup>71</sup> and Dpo4<sup>65</sup> are consistent with our values for monomeric assembly at room temperature, but those studies did not test higher concentrations required for multimeric assemblies.

A comparison of the DNA binding affinities of monomeric Dpo1 and Dpo4 shows that binding affinity is only slightly more favorable for monomeric Dpo1 across all temperature ranges but becomes more selective at physiological temperatures (Figure 6 and Figure S5 of the Supporting Information). The free energy change for binding the first molecule of Dpo1 decreases steadily with temperature up to at least ~65 °C, where binding is preferred by approximately  $-0.8 \text{ kcal mol}^{-1}$  over Dpo4. Dpo4, on the other hand, has a free energy binding minimum around 50 °C, disfavoring binding to undamaged DNA in the presence of Dpo1. Dpo4 is smaller and known to have a more open active site than typical B-family polymerases, exists in two distinct conformations, and has subtle repositioning of active site residues upon binding.<sup>18,44,72,73</sup> The little finger domain and associated linker in particular seem to be most important for stable binding to DNA. On the other hand, the binding affinity of Dpo1 for DNA is more favorable at higher temperatures, consistent with formation of a tight closed conformation on DNA, resulting in stronger DNA stabilizing ability and/or annealing noted previously.<sup>74</sup>

There is a larger differential in the free energies of binding of the oligomeric forms of the polymerases (trimeric Dpo1 or dimeric Dpo4) (Figure 6 and Figure S5 of the Supporting Information) than for the monomeric forms. The  $\Delta G^\circ$  for formation of a trimeric Dpo1 complex is much more favorable than that for formation of a dimeric Dpo4 complex. The difference in binding energies becomes even more exaggerated at higher temperatures, thus increasingly favoring the trimeric Dpo1 complex at physiological temperatures. At 64 °C, binding of trimeric Dpo1 is enormously favored (by approximately  $-9.3 \text{ kcal/mol}$ ) over dimeric Dpo4. The slight preference for binding



primer–template substrates by the Dpo1 monomer (over that of the Dpo4 monomer) will lead to trimeric Dpo1 complex formation, thus selecting against Dpo4 binding.

**Formation of Both Monomeric and Oligomeric Polymerase–DNA Complexes Produces Large Negative  $\Delta C_p^\circ$  Values.** Among the thermodynamic parameters ( $\Delta G$ ,  $\Delta H$ ,  $\Delta S$ ,  $\Delta C_p$ , and volume),  $\Delta C_p$  is one of the least well-known, but potentially the most informative with respect to extracting molecular information about specificity. Because  $\Delta C_p$  was first analyzed for protein folding, the working hypothesis was that the net negative  $\Delta C_p$  reflected primarily the burial of nonpolar surface area.<sup>46,50</sup> However, a number of studies on site-specific protein–DNA complexes have shown large deficits between the  $\Delta C_p^{\text{ASA}}$  values predicted from surface burial and experimental  $\Delta C_p^\circ$  values.<sup>29,30,35,49,52–54,56</sup> In addition to desolvation of the nonpolar surface upon binding, other factors such as restriction of conformational–vibrational motions of the macromolecules, interfacial waters, and linkage of other binding equilibria (protonation, cation, and anion binding, and conformational changes) contribute to the protein–DNA binding reaction and can potentially account for the deficit between  $\Delta C_p^{\text{ASA}}$  and  $\Delta C_p^\circ$ .<sup>29,30,75–82</sup> Although a strongly negative  $\Delta C_p^\circ$  value has generally been considered a key signature of sequence-specific DNA–protein interactions,<sup>29</sup> large negative values of  $\Delta C_p^\circ$  have also been observed for the formation of interfaces with a high degree of structural complementarity between DNA polymerases and their primer–template substrates.<sup>31,32,83,84</sup>

In the absence of appropriate monomeric or oligomeric polymerase–DNA structures, contributions of surface area burial cannot be directly assessed. The only appropriate data set is for a monomeric Dpo4–DNA structure, which underestimates the contributions of buried surface area ( $\Delta C_p^{\text{ASA}} = -0.29 \text{ kcal mol}^{-1} \text{ K}^{-1}$ ) to the experimental value. The  $\Delta C_p^\circ$  values are similar for monomeric Dpo1 ( $-0.43 \text{ kcal mol}^{-1} \text{ K}^{-1}$ ) and Dpo4 ( $-0.68 \text{ kcal mol}^{-1} \text{ K}^{-1}$ ) but significantly more negative than the  $\Delta C_p^{\text{ASA}}$  value, suggesting that other factors in addition to surface area burial contribute to the experimental  $\Delta C_p^\circ$  values.

Because we have been able to monitor the sequential steps in polymerase binding, we have also found that the  $\Delta C_p^\circ$  values for assembly of trimeric Dpo1 and dimeric Dpo4 complexes are strongly negative, suggesting that structure-specific binding is occurring during formation of these oligomeric DNA complexes as well. The sign and magnitude of the  $\Delta C_p^\circ$  values for formation of Dpo1 and Dpo4 oligomers are consistent with other specific dimerization<sup>85</sup> or binary protein binding events.<sup>86–88</sup> No structural information is available for an oligomeric Dpo1 complex, nor can we be certain of the molecular arrangement of a dimeric Dpo4 complex, which makes calculation of buried surface area difficult. Nevertheless, exclusion of water molecules, favorable surface interactions between the polymerase molecules, and restriction of configurational freedom within the oligomeric complex are consistent with the magnitudes for the oligomeric polymerase–DNA  $\Delta C_p^\circ$  values. Therefore, many of the factors discussed above may contribute to the strongly negative  $\Delta C_p^\circ$  values observed for the formation of trimeric Dpo1 and dimeric Dpo4 complexes with primer–template DNA substrates.

**Oligomeric DNA Polymerases Have Increased Activities and Processivities.** Generally, processivity is thought to be a temperature-independent parameter, although slight decreases in processivity with an increase in temperature have been noted for the telomerase enzyme.<sup>89</sup> DNA polymerases

alone are fairly distributive enzymes unless accompanied by their respective circular clamp proteins that can increase processivity from <20 to >10000 bases.<sup>90</sup> Previously, we found that the processivity of Dpo1 was dependent on concentration, such that that trimeric complex had a much greater processivity ( $\sim 1000$  bases) than the monomer at  $60^\circ \text{C}$ .<sup>20</sup> We have now shown that the processivity for both Dpo1 and Dpo4 increases with temperature. An increase in processivity with temperature was noted for both monomeric and oligomeric complexes of Dpo1 and Dpo4, although the effect was more dramatic for the oligomeric states. Trimeric Dpo1 was 4–5-fold more processive than monomeric Dpo1; dimeric Dpo4 was significantly more processive than monomeric Dpo4, but the processivity of trimeric Dpo1 was >15-fold greater than that of dimeric Dpo4 at higher temperatures. Even though Dpo4 is generally considered to be a distributive enzyme, the increased affinities for binding DNA noted with increasing temperatures and concentrations also increase the processivity. We reason that for Dpo1 and Dpo4, a more tightly bound monomeric or oligomeric complex promotes greater processivities at higher temperatures. For Dpo1, the affinity for DNA generally increases with temperature, and formation of a trimeric Dpo1 reduces the off rate of the complex from DNA over monomeric Dpo1,<sup>20</sup> explaining the larger processivity values. The combination of the higher intrinsic processivity for monomeric Dpo1 compared with that of Dpo4, as well as increased binding affinity at higher temperatures of the Dpo1 trimer, contributes to the enzymatic activity resulting in high trimeric Dpo1 processivity. In fact, phi29 is the only other characterized DNA polymerase with a greater processivity value and acts analogously by topologically encircling the DNA template.<sup>91,92</sup>

The increased binding affinity of Dpo4 for DNA also correlates well with increasing processivity up to  $60^\circ \text{C}$ . At  $70^\circ \text{C}$ , the processivity decreases slightly, consistent with the measured affinity values. Previously, when high concentrations of Dpo4 were used, an increase in the length of product synthesized was observed, suggesting that either faster repeated binding was occurring in the absence of trap or cooperation between molecules at higher concentrations afforded greater processivity.<sup>73</sup> The authors implicated the little finger domain of Dpo4 in maintaining moderate processivity by creating a closed more stable enzyme complex on DNA. The conformational change in the little finger domain is considered to be the rate-limiting step and occurs both before and after chemistry.<sup>23,93</sup> Kinetic experiments have shown that of the seven steps within the catalytic cycle for a single nucleotide incorporation event, the conformational change step that precedes chemistry is most affected by the temperature increasing 20-fold from  $37$  to  $56^\circ \text{C}$ .<sup>59</sup> Moreover, the little finger domains are in the proximity of one another in a variety of dimeric and tetrameric Dpo4 crystal structures, including our cross-linking model in Figure 1B, suggesting that dimerization may stabilize a closed complex, decrease the off rate, and increase the rate of rate-limiting conformational change step to positively affect processivity.

Clearly, a tightly bound trimeric Dpo1 complex will increase the speed and processivity of polymerization and may be utilized in various genomic maintenance applications. At  $75^\circ \text{C}$ , binding of Dpo4 will be disfavored on undamaged primer–template substrates where Dpo1 is directing synthesis. Selection and increased processivity will also be provided through interactions with the processivity clamp, SsoPCNA123, but the affinities of Dpo1 for PCNA2<sup>94</sup> and Dpo4 for PCNA1<sup>95</sup> are

very similar (M. A. Trakselis, unpublished observations). Switching from Dpo1 to Dpo4 will depend on a change in the thermodynamics of binding due to either polymerase stalling, repeated shuttling between polymerase and exonuclease sites, detection of DNA damage, or a change in the local concentrations. In those cases, binding of Dpo4 would become preferred. It has been recently estimated that the concentration of Dpo1 is at least 1 order of magnitude greater than that of Dpo4 in the cell,<sup>63</sup> suggesting that Dpo1 will be preferentially bound and will have a significant population of trimer at the replication fork. Interestingly, mRNA levels of Dpo1 decrease when cells are exposed to DNA damage in favor of Dpo4 and another B-family DNA polymerase (Dpo2),<sup>96,97</sup> suggesting that equilibrium changes will direct appropriate binding of the required DNA polymerase.

Although the oligomeric state of Dpo1 modulates both the speed and processivity of replication, the biological role of a dimeric Dpo4 remains elusive. Because of only slight increases in biochemical activity, we would predict that a dimeric Dpo4 would not be essential for cellular catalysis, but rather in either increasing the concentration of DNA polymerases at sites of DNA damage or stabilizing the closed conformational state promoting catalysis. Accurate and efficient DNA replication at high temperatures requires minimal differences in the thermodynamics of DNA polymerase binding to DNA for easy exchange of enzymes for uninterrupted synthesis. This thermodynamic compensation will be affected by small changes in the cellular equilibria that direct formation of higher-order protein complexes that promote a variety of genomic maintenance activities. The detection of multimeric polymerase complexes for both Dpo1 and Dpo4 suggests a possible mechanism for exchange, whereby direct interactions between polymerases maintain high local concentrations at the replication fork that can thermodynamically switch binding modes when required.

## ■ ASSOCIATED CONTENT

### ■ Supporting Information

Simulation data for concentration- and temperature-dependent assembly of Dpo1 and Dpo4 on DNA, thermodynamic parameters for Dpo1 and Dpo4 binding to DNA (Tables S1 and S2, respectively), AUC data of Dpo1 and Dpo4 alone (Figure S1), AU-FDS temperature-dependent data of Dpo1 and Dpo4 bound to DNA (Figure S2), examples of anisotropy fits (Figure S3), fitted thermodynamic parameters for Dpo1 and Dpo4 binding to DNA (Figure S4), thermodynamic differences between Dpo1 and Dpo4 binding to DNA (Figure S5), Dpo1 polymerization rate at different temperatures (Figure S6), and Dpo4 processivity at different temperatures (Figure S7). This material is available free of charge via the Internet at <http://pubs.acs.org>.

## ■ AUTHOR INFORMATION

### Corresponding Author

\*L.J.-J.: 4249 Fifth Ave., 320 Clapp Hall, Pittsburgh, PA 15260; telephone, (412) 624-4969; e-mail, [ljen@pitt.edu](mailto:ljen@pitt.edu). M.A.T.: 219 Parkman Ave., 801 Chevron, Pittsburgh, PA 15260; telephone, (412) 624-1204; fax, (412) 624-8611; e-mail, [mtraksel@pitt.edu](mailto:mtraksel@pitt.edu).

### Funding

This work was supported by startup funds from the University of Pittsburgh, Department of Chemistry (M.A.T.), a Research

Scholar Grant (RSG-11-049-01-DMC) to M.A.T. from the American Cancer Society, and National Institutes of Health MERIT Award 5R37-GM29207 to L.J.-J. Funding for the analytical ultracentrifuge was provided by the National Science Foundation (NSF, BIR-9876582) and the National Institutes of Health (NIH, 1R01GM6283601) to T.M.L.

### Notes

The authors declare no competing financial interest.

## ■ ACKNOWLEDGMENTS

We thank Roger Woodgate for providing the pET22b-Dpo4 expression plasmid. We also thank Reza Salari and Lillian Chong for help in calculating buried surface areas for Dpo4 and DNA.

## ■ ABBREVIATIONS

ITC, isothermal titration calorimetry;  $\Delta C_p^\circ$ , change in heat capacity;  $\Delta C_p^{ASA}$ , surface area-calculated heat capacity;  $\Delta A_p$ , change in polar surface area;  $\Delta A_{np}$ , change in nonpolar surface area;  $K_d$ , dissociation constant;  $K_{app}$ , apparent association constant;  $\Delta G^\circ$ , binding free energy;  $\Delta H^\circ$ , change in enthalpy;  $\Delta S^\circ$ , change in entropy;  $n$ , stoichiometry; AUC, analytical ultracentrifugation; AU-FDS, analytical ultracentrifugation fluorescence-detected sedimentation;  $D_v$ , diffusion coefficient;  $s$ , sedimentation coefficient; EMSA, electrophoretic mobility shift assay;  $k_{pol}$ , rate constant of synthesis for the next catalytic step;  $k_{dis}$ , rate constant of dissociation from the template; nt, nucleotide.

## ■ REFERENCES

- (1) Burgers, P. M., Koonin, E. V., Bruford, E., Blanco, L., Burtis, K. C., Christman, M. F., Copeland, W. C., Friedberg, E. C., Hanaoka, F., Hinkle, D. C., Lawrence, C. W., Nakanishi, M., Ohmori, H., Prakash, L., Prakash, S., Reynaud, C. A., Sugino, A., Todo, T., Wang, Z., Weill, J. C., and Woodgate, R. (2001) Eukaryotic DNA polymerases: Proposal for a revised nomenclature. *J. Biol. Chem.* 276, 43487–43490.
- (2) Lange, S. S., Takata, K., and Wood, R. D. (2011) DNA polymerases and cancer. *Nat. Rev. Cancer* 11, 96–110.
- (3) Nishida, H., Mayanagi, K., Kiyonari, S., Sato, Y., Oyama, T., Ishino, Y., and Morikawa, K. (2009) Structural determinant for switching between the polymerase and exonuclease modes in the PCNA-replicative DNA polymerase complex. *Proc. Natl. Acad. Sci. U.S.A.* 106, 20693–20698.
- (4) Purohit, V., Grindley, N. D., and Joyce, C. M. (2003) Use of 2-aminopurine fluorescence to examine conformational changes during nucleotide incorporation by DNA polymerase I (Klenow fragment). *Biochemistry* 42, 10200–10211.
- (5) Ishmael, F. T., Trakselis, M. A., and Benkovic, S. J. (2003) Protein-protein interactions in the bacteriophage T4 replisome. The leading strand holoenzyme is physically linked to the lagging strand holoenzyme and the primosome. *J. Biol. Chem.* 278, 3145–3152.
- (6) Jezewska, M. J., Rajendran, S., and Bujalowski, W. (1998) Transition between different binding modes in rat DNA polymerase  $\beta$ -ssDNA complexes. *J. Mol. Biol.* 284, 1113–1131.
- (7) Tang, K. H., Niebuhr, M., Aulabaugh, A., and Tsai, M. D. (2008) Solution structures of 2:1 and 1:1 DNA polymerase-DNA complexes probed by ultracentrifugation and small-angle X-ray scattering. *Nucleic Acids Res.* 36, 849–860.
- (8) Jezewska, M. J., Bujalowski, P. J., and Bujalowski, W. (2007) Interactions of the DNA polymerase X from African swine fever virus with gapped DNA substrates. Quantitative analysis of functional structures of the formed complexes. *Biochemistry* 46, 12909–12924.
- (9) Tang, K. H., and Tsai, M. D. (2008) Structure and function of 2:1 DNA polymerase-DNA complexes. *J. Cell. Physiol.* 216, 315–320.

- (10) McInerney, P., Johnson, A., Katz, F., and O'Donnell, M. (2007) Characterization of a triple DNA polymerase replisome. *Mol. Cell* 27, 527–538.
- (11) Yang, J., Zhuang, Z., Roccasecca, R. M., Trakselis, M. A., and Benkovic, S. J. (2004) The dynamic processivity of the T4 DNA polymerase during replication. *Proc. Natl. Acad. Sci. U.S.A.* 101, 8289–8294.
- (12) Loparo, J. J., Kulczyk, A. W., Richardson, C. C., and van Oijen, A. M. (2011) Simultaneous single-molecule measurements of phage T7 replisome composition and function reveal the mechanism of polymerase exchange. *Proc. Natl. Acad. Sci. U.S.A.* 108, 3584–3589.
- (13) Koonin, E. V., Mushegian, A. R., Galperin, M. Y., and Walker, D. R. (1997) Comparison of archaeal and bacterial genomes: Computer analysis of protein sequences predicts novel functions and suggests a chimeric origin for the archaea. *Mol. Microbiol.* 25, 619–637.
- (14) Barry, E. R., and Bell, S. D. (2006) DNA replication in the archaea. *Microbiol. Mol. Biol. Rev.* 70, 876–887.
- (15) Tahirov, T. H., Makarova, K. S., Rogozin, I. B., Pavlov, Y. I., and Koonin, E. V. (2009) Evolution of DNA polymerases: An inactivated polymerase-exonuclease module in Pol  $\epsilon$  and a chimeric origin of eukaryotic polymerases from two classes of archaeal ancestors. *Biol. Direct* 4, 11.
- (16) Savino, C., Federici, L., Johnson, K. A., Vallone, B., Nastopoulos, V., Rossi, M., Pisani, F. M., and Tsernoglou, D. (2004) Insights into DNA replication: The crystal structure of DNA polymerase B1 from the archaeon *Sulfolobus solfataricus*. *Structure* 12, 2001–2008.
- (17) Boudsocq, F., Iwai, S., Hanaoka, F., and Woodgate, R. (2001) *Sulfolobus solfataricus* P2 DNA polymerase IV (Dpo4): An archaeal DinB-like DNA polymerase with lesion-bypass properties akin to eukaryotic pol  $\eta$ . *Nucleic Acids Res.* 29, 4607–4616.
- (18) Ling, H., Boudsocq, F., Woodgate, R., and Yang, W. (2001) Crystal structure of a Y-family DNA polymerase in action: A mechanism for error-prone and lesion-bypass replication. *Cell* 107, 91–102.
- (19) Kokoska, R. J., Bebenek, K., Boudsocq, F., Woodgate, R., and Kunkel, T. A. (2002) Low fidelity DNA synthesis by a Y-family DNA polymerase due to misalignment in the active site. *J. Biol. Chem.* 277, 19633–19638.
- (20) Mikhelkin, A. L., Lin, H. K., Mehta, P., Jen-Jacobson, L., and Trakselis, M. A. (2009) A trimeric DNA polymerase complex increases the native replication processivity. *Nucleic Acids Res.* 37, 7194–7205.
- (21) Brown, J. A., and Suo, Z. (2009) Elucidating the kinetic mechanism of DNA polymerization catalyzed by *Sulfolobus solfataricus* P2 DNA polymerase B1. *Biochemistry* 48, 7502–7511.
- (22) Fiala, K. A., Hypes, C. D., and Suo, Z. (2007) Mechanism of abasic lesion bypass catalyzed by a Y-family DNA polymerase. *J. Biol. Chem.* 282, 8188–8198.
- (23) Fiala, K. A., and Suo, Z. (2004) Mechanism of DNA polymerization catalyzed by *Sulfolobus solfataricus* P2 DNA polymerase IV. *Biochemistry* 43, 2116–2125.
- (24) Fiala, K. A., and Suo, Z. (2004) Pre-steady-state kinetic studies of the fidelity of *Sulfolobus solfataricus* P2 DNA polymerase IV. *Biochemistry* 43, 2106–2115.
- (25) Zang, H., Irimia, A., Choi, J. Y., Angel, K. C., Loukachevitch, L. V., Egli, M., and Guengerich, F. P. (2006) Efficient and high fidelity incorporation of dCTP opposite 7,8-dihydro-8-oxodeoxyguanosine by *Sulfolobus solfataricus* DNA polymerase Dpo4. *J. Biol. Chem.* 281, 2358–2372.
- (26) Zang, H., Goodenough, A. K., Choi, J. Y., Irimia, A., Loukachevitch, L. V., Kozekov, I. D., Angel, K. C., Rizzo, C. J., Egli, M., and Guengerich, F. P. (2005) DNA adduct bypass polymerization by *Sulfolobus solfataricus* DNA polymerase Dpo4: Analysis and crystal structures of multiple base pair substitution and frameshift products with the adduct 1,N2-ethenoguanine. *J. Biol. Chem.* 280, 29750–29764.
- (27) Sakofsky, C. J., Foster, P. L., and Grogan, D. W. (2012) Roles of the Y-family DNA polymerase Dbh in accurate replication of the *Sulfolobus* genome at high temperature. *DNA Repair* 11, 391–400.
- (28) De Felice, M., Medagli, B., Esposito, L., De Falco, M., Pucci, B., Rossi, M., Gruz, P., Nohmi, T., and Pisani, F. M. (2007) Biochemical evidence of a physical interaction between *Sulfolobus solfataricus* B-family and Y-family DNA polymerases. *Extremophiles* 11, 277–282.
- (29) Jen-Jacobson, L., Engler, L. E., and Jacobson, L. A. (2000) Structural and thermodynamic strategies for site-specific DNA binding proteins. *Structure* 8, 1015–1023.
- (30) Jen-Jacobson, L., Engler, L. E., Ames, J. T., Kurpiewski, M. R., and Grigorescu, A. (2000) Thermodynamic parameters of specific and nonspecific protein-DNA binding. *Supramol. Chem.* 12, 143–160.
- (31) Datta, K., and LiCata, V. J. (2003) Thermodynamics of the binding of *Thermus aquaticus* DNA polymerase to primed-template DNA. *Nucleic Acids Res.* 31, 5590–5597.
- (32) Datta, K., Wowor, A. J., Richard, A. J., and LiCata, V. J. (2006) Temperature dependence and thermodynamics of Klenow polymerase binding to primed-template DNA. *Biophys. J.* 90, 1739–1751.
- (33) Takeda, Y., Ross, P. D., and Mudd, C. P. (1992) Thermodynamics of Cro protein-DNA interactions. *Proc. Natl. Acad. Sci. U.S.A.* 89, 8180–8184.
- (34) Lundback, T., Hansson, H., Knapp, S., Ladenstein, R., and Hard, T. (1998) Thermodynamic characterization of non-sequence-specific DNA-binding by the Sso7d protein from *Sulfolobus solfataricus*. *J. Mol. Biol.* 276, 775–786.
- (35) Ladbury, J. E., Wright, J. G., Sturtevant, J. M., and Sigler, P. B. (1994) A thermodynamic study of the trp repressor-operator interaction. *J. Mol. Biol.* 238, 669–681.
- (36) Eom, S. H., Wang, J., and Steitz, T. A. (1996) Structure of *Taq* polymerase with DNA at the polymerase active site. *Nature* 382, 278–281.
- (37) Beese, L. S., Derbyshire, V., and Steitz, T. A. (1993) Structure of DNA polymerase I Klenow fragment bound to duplex DNA. *Science* 260, 352–355.
- (38) Studier, F. W. (2005) Protein production by auto-induction in high density shaking cultures. *Protein Expression Purif.* 41, 207–234.
- (39) Pierce, M. M., Raman, C. S., and Nall, B. T. (1999) Isothermal titration calorimetry of protein-protein interactions. *Methods* 19, 213–221.
- (40) Schuck, P. (2000) Size-distribution analysis of macromolecules by sedimentation velocity ultracentrifugation and Lamm equation modeling. *Biophys. J.* 78, 1606–1619.
- (41) Laue, T. M., Saha, B. D., Ridgeway, T. M., and Pelletier, S. L. (1992) Computer-aided interpretation of analytical sedimentation data for proteins. In *Analytical Ultracentrifugation in Biochemistry and Polymer Science* (Harding, S. E., Ed.) pp 90–125, Royal Society of Chemistry, Cambridge, U.K.
- (42) Schuck, P. (2003) On the analysis of protein self-association by sedimentation velocity analytical ultracentrifugation. *Anal. Biochem.* 320, 104–124.
- (43) Marras, S. A. (2006) Selection of fluorophore and quencher pairs for fluorescent nucleic acid hybridization probes. *Methods Mol. Biol.* 335, 3–16.
- (44) Wong, J. H., Fiala, K. A., Suo, Z., and Ling, H. (2008) Snapshots of a Y-family DNA polymerase in replication: Substrate-induced conformational transitions and implications for fidelity of Dpo4. *J. Mol. Biol.* 379, 317–330.
- (45) Sanner, M. F., Olson, A. J., and Spohner, J. C. (1996) Reduced surface: An efficient way to compute molecular surfaces. *Biopolymers* 38, 305–320.
- (46) Spolar, R. S., Livingstone, J. R., and Record, M. T. (1992) Use of liquid hydrocarbon and amide transfer data to estimate contributions to thermodynamic functions of protein folding from the removal of nonpolar and polar surface from water. *Biochemistry* 31, 3947–3955.
- (47) Zhang, H., Eoff, R. L., Kozekov, I. D., Rizzo, C. J., Egli, M., and Guengerich, F. P. (2009) Structure-function relationships in miscoding by *Sulfolobus solfataricus* DNA polymerase Dpo4: Guanine N2,N2-dimethyl substitution produces inactive and miscoding polymerase complexes. *J. Biol. Chem.* 284, 17687–17699.



- (48) Kingsbury, J. S., and Laue, T. M. (2011) Fluorescence-detected sedimentation in dilute and highly concentrated solutions. *Methods Enzymol.* 492, 283–304.
- (49) Ha, J. H., Spolar, R. S., and Record, M. T., Jr. (1989) Role of the hydrophobic effect in stability of site-specific protein-DNA complexes. *J. Mol. Biol.* 209, 801–816.
- (50) Spolar, R. S., and Record, M. T., Jr. (1994) Coupling of local folding to site-specific binding of proteins to DNA. *Science* 263, 777–784.
- (51) Lazaridis, T., and Karplus, M. (1999) Heat capacity and compactness of denatured proteins. *Biophys. Chem.* 78, 207–217.
- (52) Petri, V., Hsieh, M., and Brenowitz, M. (1995) Thermodynamic and kinetic characterization of the binding of the TATA binding protein to the adenovirus E4 promoter. *Biochemistry* 34, 9977–9984.
- (53) Berger, C., Jelesarov, I., and Bosshard, H. R. (1996) Coupled folding and site-specific binding of the GCN4-bZIP transcription factor to the AP-1 and ATF/CREB DNA sites studied by microcalorimetry. *Biochemistry* 35, 14984–14991.
- (54) Lundback, T., Cairns, C., Gustafsson, J. A., Carlstedt-Duke, J., and Hard, T. (1993) Thermodynamics of the glucocorticoid receptor-DNA interaction: Binding of wild-type GR DBD to different response elements. *Biochemistry* 32, 5074–5082.
- (55) Morton, C. J., and Ladbury, J. E. (1996) Water-mediated protein-DNA interactions: The relationship of thermodynamics to structural detail. *Protein Sci.* 5, 2115–2118.
- (56) Jen-Jacobson, L., and Jacobson, L. A. (2008) Role of Water and Effects of Small Ions in Site-specific Protein-DNA Interactions. In *Protein-Nucleic Acid Interactions: Structural Biology*, Chapter 2, pp 13–46, The Royal Society of Chemistry, Cambridge, U.K.
- (57) Fairfield, F. R., Newport, J. W., Dolejsi, M. K., and von Hippel, P. H. (1983) On the processivity of DNA replication. *J. Biomol. Struct. Dyn.* 1, 715–727.
- (58) Eoff, R. L., Sanchez-Ponce, R., and Guengerich, F. P. (2009) Conformational changes during nucleotide selection by *Sulfolobus solfataricus* DNA polymerase Dpo4. *J. Biol. Chem.* 284, 21090–21099.
- (59) Fiala, K. A., Sherrer, S. M., Brown, J. A., and Suo, Z. (2008) Mechanistic consequences of temperature on DNA polymerization catalyzed by a Y-family DNA polymerase. *Nucleic Acids Res.* 36, 1990–2001.
- (60) Fiala, K. A., and Suo, Z. (2007) Sloppy bypass of an abasic lesion catalyzed by a Y-family DNA polymerase. *J. Biol. Chem.* 282, 8199–8206.
- (61) Vaisman, A., Ling, H., Woodgate, R., and Yang, W. (2005) Fidelity of Dpo4: Effect of metal ions, nucleotide selection and pyrophosphorolysis. *EMBO J.* 24, 2957–2967.
- (62) Ling, H., Boudsocq, F., Woodgate, R., and Yang, W. (2004) Snapshots of replication through an abasic lesion; structural basis for base substitutions and frameshifts. *Mol. Cell* 13, 751–762.
- (63) Choi, J. Y., Eoff, R. L., Pence, M. G., Wang, J., Martin, M. V., Kim, E. J., Folkmann, L. M., and Guengerich, F. P. (2011) Roles of the four DNA polymerases of the crenarchaeon *Sulfolobus solfataricus* and accessory proteins in DNA replication. *J. Biol. Chem.* 286, 31180–31193.
- (64) Sherrer, S. M., Brown, J. A., Pack, L. R., Jasti, V. P., Fowler, J. D., Basu, A. K., and Suo, Z. (2009) Mechanistic studies of the bypass of a bulky single-base lesion catalyzed by a Y-family DNA polymerase. *J. Biol. Chem.* 284, 6379–6388.
- (65) Fiala, K. A., Brown, J. A., Ling, H., Kshetry, A. K., Zhang, J., Taylor, J. S., Yang, W., and Suo, Z. (2007) Mechanism of template-independent nucleotide incorporation catalyzed by a template-dependent DNA polymerase. *J. Mol. Biol.* 365, 590–602.
- (66) Eoff, R. L., Stafford, J. B., Szekely, J., Rizzo, C. J., Egli, M., Guengerich, F. P., and Marnett, L. J. (2009) Structural and functional analysis of *Sulfolobus solfataricus* Y-family DNA polymerase Dpo4-catalyzed bypass of the malondialdehyde-deoxyguanosine adduct. *Biochemistry* 48, 7079–7088.
- (67) Irimia, A., Eoff, R. L., Pallan, P. S., Guengerich, F. P., and Egli, M. (2007) Structure and activity of Y-class DNA polymerase Dpo4 from *Sulfolobus solfataricus* with templates containing the hydrophobic thymine analog 2,4-difluorotoluene. *J. Biol. Chem.* 282, 36421–36433.
- (68) Silvian, L. F., Toth, E. A., Pham, P., Goodman, M. F., and Ellenberger, T. (2001) Crystal structure of a DinB family error-prone DNA polymerase from *Sulfolobus solfataricus*. *Nat. Struct. Biol.* 8, 984–989.
- (69) Wilson, R. C., and Pata, J. D. (2008) Structural insights into the generation of single-base deletions by the Y family DNA polymerase dbh. *Mol. Cell* 29, 767–779.
- (70) Pata, J. D. (2010) Structural diversity of the Y-family DNA polymerases. *Biochim. Biophys. Acta* 1804, 1124–1135.
- (71) Gruz, P., Shimizu, M., Pisani, F. M., De, F. M., Kanke, Y., and Nohmi, T. (2003) Processing of DNA lesions by archaeal DNA polymerases from *Sulfolobus solfataricus*. *Nucleic Acids Res.* 31, 4024–4030.
- (72) Xu, C., Maxwell, B. A., Brown, J. A., Zhang, L., and Suo, Z. (2009) Global conformational dynamics of a Y-family DNA polymerase during catalysis. *PLoS Biol.* 7, e1000225.
- (73) Boudsocq, F., Kokoska, R. J., Plosky, B. S., Vaisman, A., Ling, H., Kunkel, T. A., Yang, W., and Woodgate, R. (2004) Investigating the role of the little finger domain of Y-family DNA polymerases in low fidelity synthesis and translesion replication. *J. Biol. Chem.* 279, 32932–32940.
- (74) Zuo, Z., Lin, H. K., and Trakselis, M. A. (2011) Strand annealing and terminal transferase activities of a B-family DNA polymerase. *Biochemistry* 50, 5379–5390.
- (75) Sturtevant, J. M. (1977) Heat capacity and entropy changes in processes involving proteins. *Proc. Natl. Acad. Sci. U.S.A.* 74, 2236–2240.
- (76) Eftink, M. R., Anusiem, A. C., and Biltonen, R. L. (1983) Enthalpy-entropy compensation and heat capacity changes for protein-ligand interactions: General thermodynamic models and data for the binding of nucleotides to ribonuclease A. *Biochemistry* 22, 3884–3896.
- (77) Peters, W. B., Edmondson, S. P., and Shriver, J. W. (2005) Effect of mutation of the Sac7d intercalating residues on the temperature dependence of DNA distortion and binding thermodynamics. *Biochemistry* 44, 4794–4804.
- (78) Kozlov, A. G., and Lohman, T. M. (2011) *E. coli* SSB tetramer binds the first and second molecules of (dT)<sub>35</sub> with heat capacities of opposite sign. *Biophys. Chem.* 159, 48–57.
- (79) Kozlov, A. G., and Lohman, T. M. (2006) Effects of monovalent anions on a temperature-dependent heat capacity change for *Escherichia coli* SSB tetramer binding to single-stranded DNA. *Biochemistry* 45, 5190–5205.
- (80) Kozlov, A. G., and Lohman, T. M. (2000) Large contributions of coupled protonation equilibria to the observed enthalpy and heat capacity changes for ssDNA binding to *Escherichia coli* SSB protein. *Proteins* 4 (Suppl.), 8–22.
- (81) Holbrook, J. A., Tsodikov, O. V., Saecker, R. M., and Record, M. T., Jr. (2001) Specific and non-specific interactions of integration host factor with DNA: Thermodynamic evidence for disruption of multiple IHF surface salt-bridges coupled to DNA binding. *J. Mol. Biol.* 310, 379–401.
- (82) Bergqvist, S., Williams, M. A., O'Brien, R., and Ladbury, J. E. (2004) Heat capacity effects of water molecules and ions at a protein-DNA interface. *J. Mol. Biol.* 336, 829–842.
- (83) Yang, Y., and LiCata, V. J. (2011) Interactions of replication versus repair DNA substrates with the Pol I DNA polymerases from *Escherichia coli* and *Thermus aquaticus*. *Biophys. Chem.* 159, 188–193.
- (84) Datta, K., Johnson, N. P., LiCata, V. J., and von Hippel, P. H. (2009) Local conformations and competitive binding affinities of single- and double-stranded primer-template DNA at the polymerization and editing active sites of DNA polymerases. *J. Biol. Chem.* 284, 17180–17193.
- (85) Filfil, R., and Chalikian, T. V. (2003) The thermodynamics of protein-protein recognition as characterized by a combination of volumetric and calorimetric techniques: The binding of turkey ovomucoid third domain to  $\alpha$ -chymotrypsin. *J. Mol. Biol.* 326, 1271–1288.

- (86) Baker, B. M., and Murphy, K. P. (1997) Dissecting the energetics of a protein-protein interaction: The binding of ovomucoid third domain to elastase. *J. Mol. Biol.* 268, 557–569.
- (87) Armstrong, K. M., Insaudo, F. K., and Baker, B. M. (2008) Thermodynamics of T-cell receptor-peptide/MHC interactions: Progress and opportunities. *J. Mol. Recognit.* 21, 275–287.
- (88) Frisch, C., Schreiber, G., Johnson, C. M., and Fersht, A. R. (1997) Thermodynamics of the interaction of barnase and barstar: Changes in free energy versus changes in enthalpy on mutation. *J. Mol. Biol.* 267, 696–706.
- (89) Sun, D., Lopez-Guajardo, C. C., Quada, J., Hurley, L. H., and Von Hoff, D. D. (1999) Regulation of catalytic activity and processivity of human telomerase. *Biochemistry* 38, 4037–4044.
- (90) Trakselis, M. A., and Benkovic, S. J. (2001) Intricacies in ATP-dependent clamp loading: Variations across replication systems. *Structure* 9, 999–1004.
- (91) Kamtekar, S., Berman, A. J., Wang, J., Lazaro, J. M., de, V. M., Blanco, L., Salas, M., and Steitz, T. A. (2006) The phi29 DNA polymerase: Protein-primer structure suggests a model for the initiation to elongation transition. *EMBO J.* 25, 1335–1343.
- (92) Blanco, L., Bernad, A., Lazaro, J. M., Martin, G., Garmendia, C., and Salas, M. (1989) Highly efficient DNA synthesis by the phage phi29 DNA polymerase. Symmetrical mode of DNA replication. *J. Biol. Chem.* 264, 8935–8940.
- (93) Beckman, J. W., Wang, Q., and Guengerich, F. P. (2008) Kinetic analysis of correct nucleotide insertion by a Y-family DNA polymerase reveals conformational changes both prior to and following phosphodiester bond formation as detected by tryptophan fluorescence. *J. Biol. Chem.* 283, 36711–36723.
- (94) Dionne, I., Nookala, R. K., Jackson, S. P., Doherty, A. J., and Bell, S. D. (2003) A heterotrimeric PCNA in the hyperthermophilic archaeon *Sulfolobus solfataricus*. *Mol. Cell* 11, 275–282.
- (95) Dionne, I., Brown, N. J., Woodgate, R., and Bell, S. D. (2008) On the mechanism of loading the PCNA sliding clamp by RFC. *Mol. Microbiol.* 68, 216–222.
- (96) Gotz, D., Paytubi, S., Munro, S., Lundgren, M., Bernander, R., and White, M. F. (2007) Responses of hyperthermophilic crenarchaea to UV irradiation. *Genome Biol.* 8, R220.
- (97) Frols, S., Gordon, P. M., Panlilio, M. A., Duggin, I. G., Bell, S. D., Sensen, C. W., and Schleper, C. (2007) Response of the hyperthermophilic archaeon *Sulfolobus solfataricus* to UV damage. *J. Bacteriol.* 189, 8708–8718.